Supporting Information

A highly stable all-in-one photocatalyst for aryl etherification: The Ni^{II} embedded covalent organic framework

Wenbo Dong,[a] Yi Yang,[a] Yonggang Xiang,*[a] Shengyao Wang,[a] Pei Wang,[a] Jianxiang Hu,[a] Li Rao*[b] and Hao Chen*[a]

[a] College of Science, Huazhong Agricultural University, Wuhan 430070, P. R. China

[b] Key Laboratory of Pesticide & Chemical Biology (CCNU), Ministry of Education, Department of Chemistry, Central China Normal University, Wuhan 430079, PR China

Table of Contents

1. General information

1.1 Reagents:

Unless otherwise noted, all the chemicals and reagents were purchased in analytical purity from commercial suppliers and used directly without further purification. 1,3,6,8-tetrakis(4-formylphenyl)pyrene (**TFPPy**),[1] and 2,2'-([2,2'-bipyridine]-5,5'-diyl)diacetonitrile (**BPYDAN**)[2] were prepared according to reported procedure. The reported sp^2c-COF_{bp} was synthesized as reported.[3]

1.2 Characterization.

^1H NMR, ^{13}C NMR and ^{19}F NMR were recorded on Bruker Advance 600 MHz, 150 MHz and 376 MHz spectrometer at 298 K, respectively, and chemical shift (δ) was reported in ppm relative to the residual solvent peaks. Peaks are reported as: s = singlet, d = doublet, t = triplet, q = quartet, m = multiplet or unresolved, with coupling constants in Hz. Preparative thin-layer chromatography (PTLC) was performed on pre-coated TLC-sheets. The reaction process was analyzed with decane as internal standard by gas chromatography (GC, Agilent 7890B). The final products were determined via High Resolution Mass Spectrometry (HRMS, Shimadzu, LCMS-8050). The diffractometer (D8 advance, Bruker, Germany) with Cu Kα radiation was used to record the powder X-ray diffraction (PXRD). The content of Ni was analyzed by inductively coupled plasma optical emission spectrometry (ICP-OES, 7800, Agilent Technologies, USA), where the sample was first digested by H_2SO_4/HNO_3 (0.8 mL/0.2 mL) solvent at 60 ^oC. The Fourier transform-infrared (FT-IR) were recorded on Nicolet 6700 spectrometer (Thermo Scientific, USA). Solid state ^{13}C cross polarization magic angle spinning (^{13}C-CP/MAS) NMR spectra were measured by Bruker Avance III HD 400 spectrometer. X-ray photoelectron spectroscopy (XPS) measurements were performed on a Thermo ESCALAB 250 spectrometer with non-monochromatic Al Kα x-rays as the excitation source and C 1s (284.8 eV) as the reference line. Transmission electron microscopy (TEM) was obtained on JEM-2100F and JEM-ARM200F. Scanning electron microscope (SEM) was performed on SU8010. N_2 adsorption and desorption isotherms were measured at 77 K using a Micromeritics ASAP 2020 system. UV-Vis diffused reflectance spectra (DRS) were measured on a Shimadzu UV-3100 spectrometer.

The X-ray absorption fine structure spectra were performed at 1W1B station in Beijing Synchrotron Radiation Facility (BSRF). The obtained XAFS data was processed in Athena (version 0.9.25) for background, pre-edge line and post-edge line calibrations. Then Fourier transformed fitting was carried out in Artemis (version 0.9.25). The k^3 weighting, k-range of 3 - 12 $Å^{-1}$ and R range of 1 - ~3 Å were used for the fitting. The model of Ni-foil, NiPc and NiO were used to calculate the simulated scattering paths. The four parameters, coordination number, bond length, Debye-Waller factor and E_0 shift (CN, R, σ^2, ΔE_0) were fitted without anyone was fixed, constrained, or correlated.

2. Structure of $sp^2c\text{-}COF_{bp}$

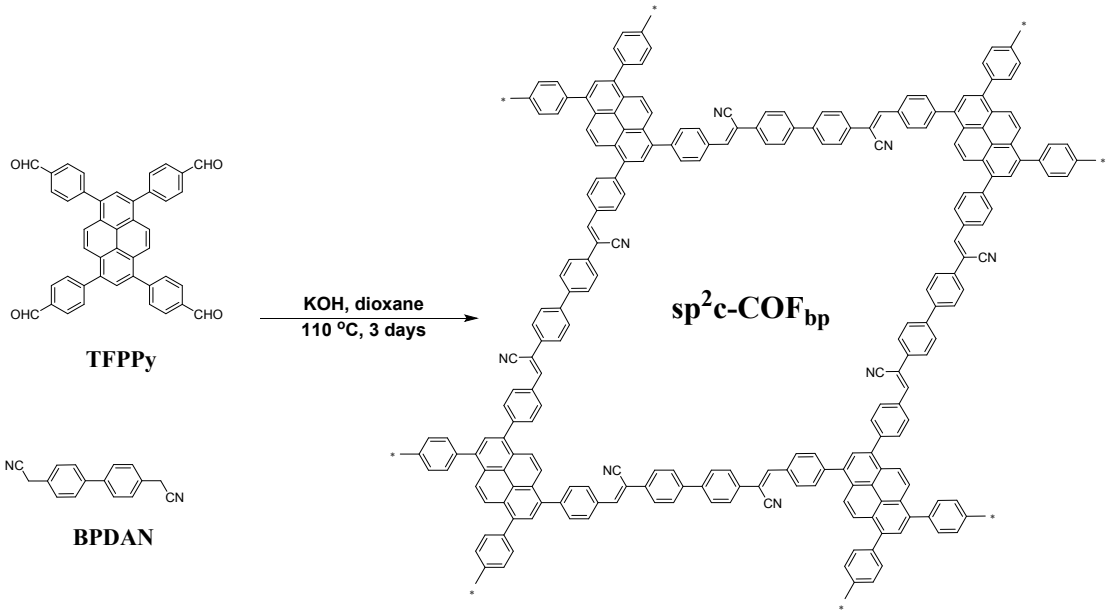

Scheme S1. Structure of $sp^2c\text{-}COF_{bp}$[3]

3. Characterizations of sp^2c-COF

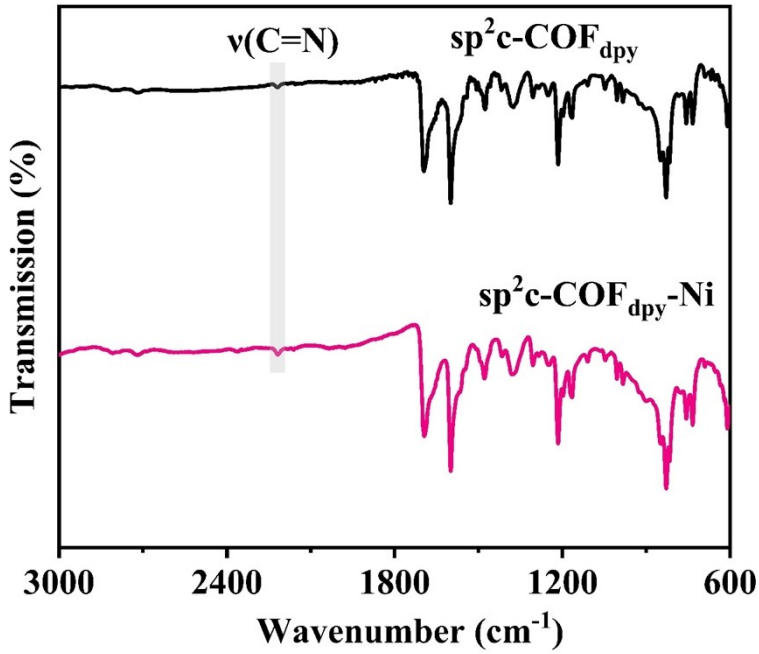

Figure S1. FT-IR spectroscopy of sp^2c-COF_{dpy} and sp^2c-COF_{dpy}-Ni.

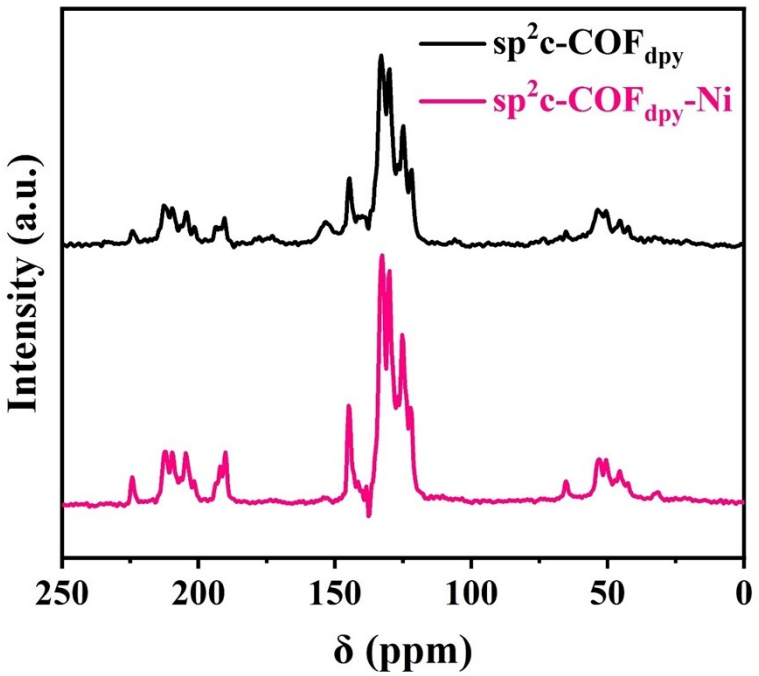

Figure S2. Solid-state ^{13}C CP/MAS NMR spectra of sp^2c-COF_{dpy} and sp^2c-COF_{dpy}-Ni.

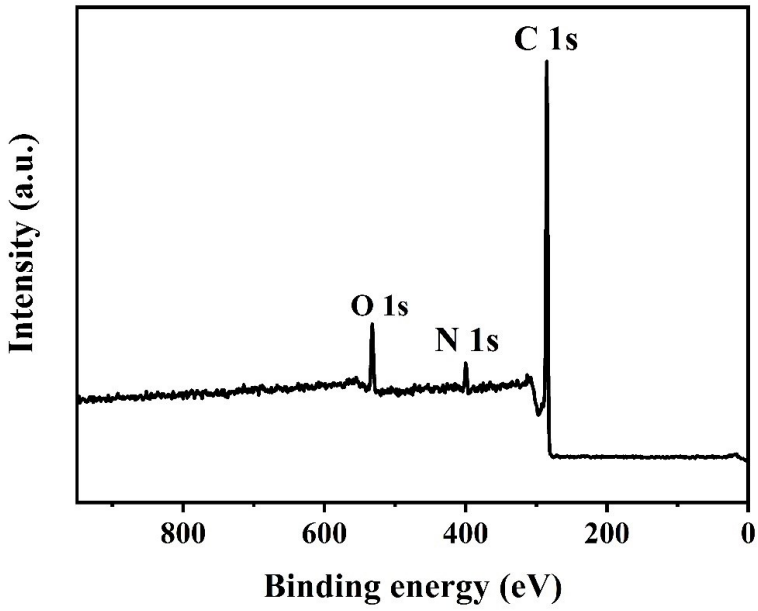

Figure S3. XPS survey spectra of sp^2c-COF_{dpy}.

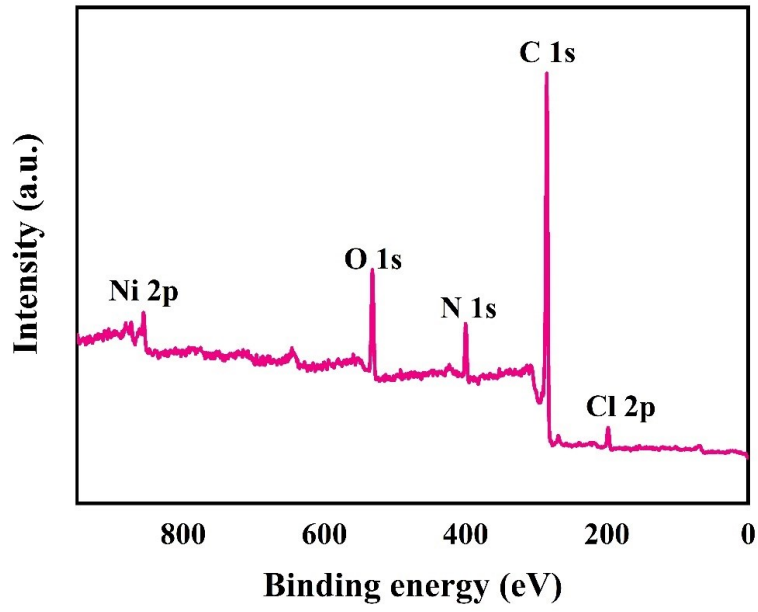

Figure S4. XPS survey spectra of sp^2c-COF_{dpy}-Ni.

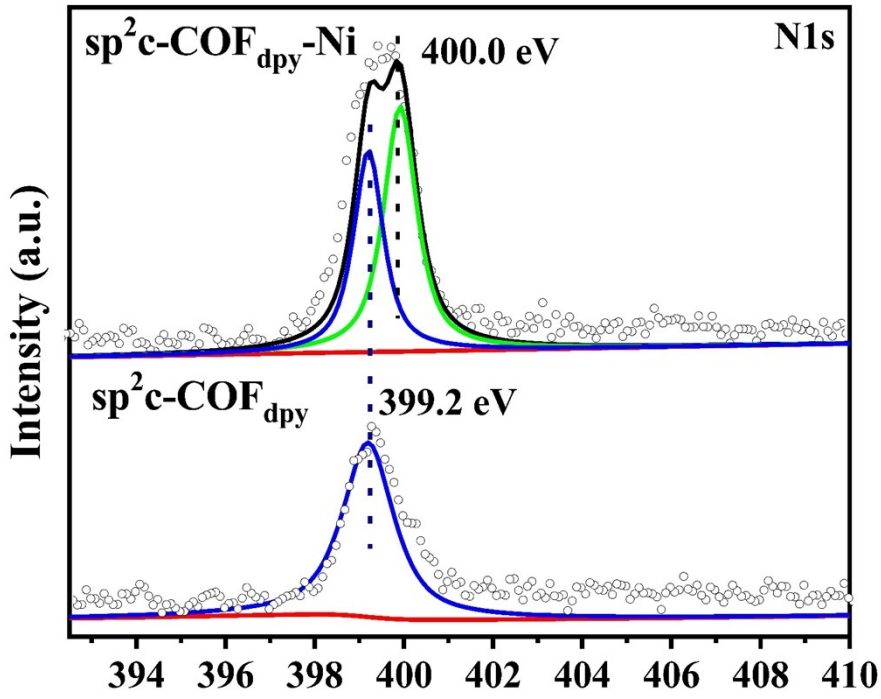

Figure S5. High-resolution N 1s XPS spectra of sp^2c-COF_{dpy} and sp^2c-COF_{dpy}-Ni.

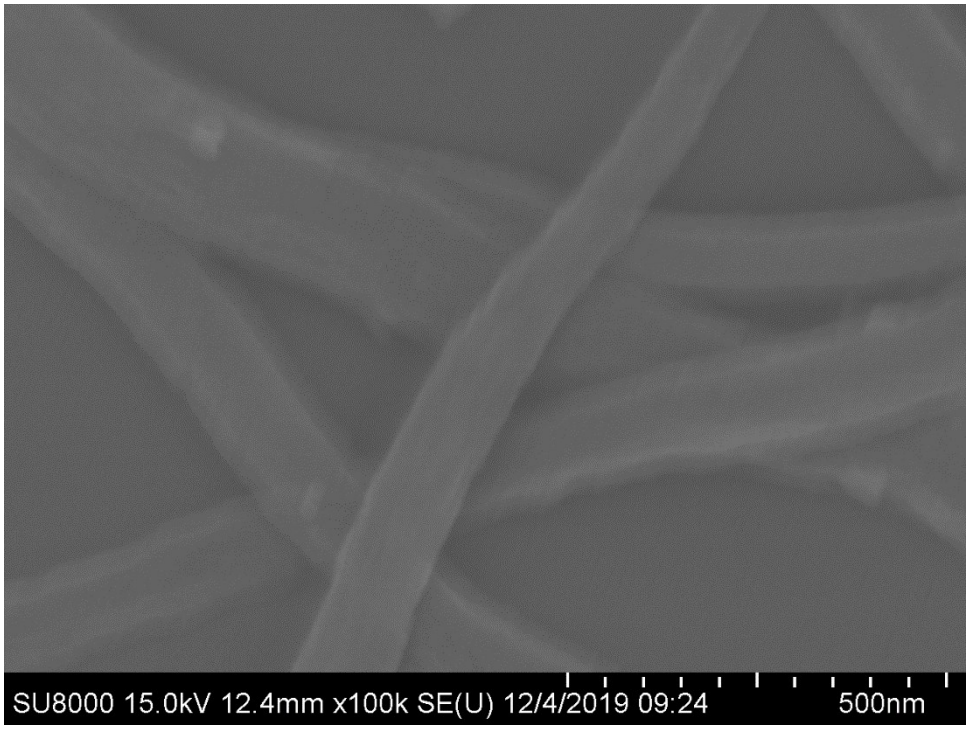

Figure S6. SEM image of sp^2c-COF_{dpy}.

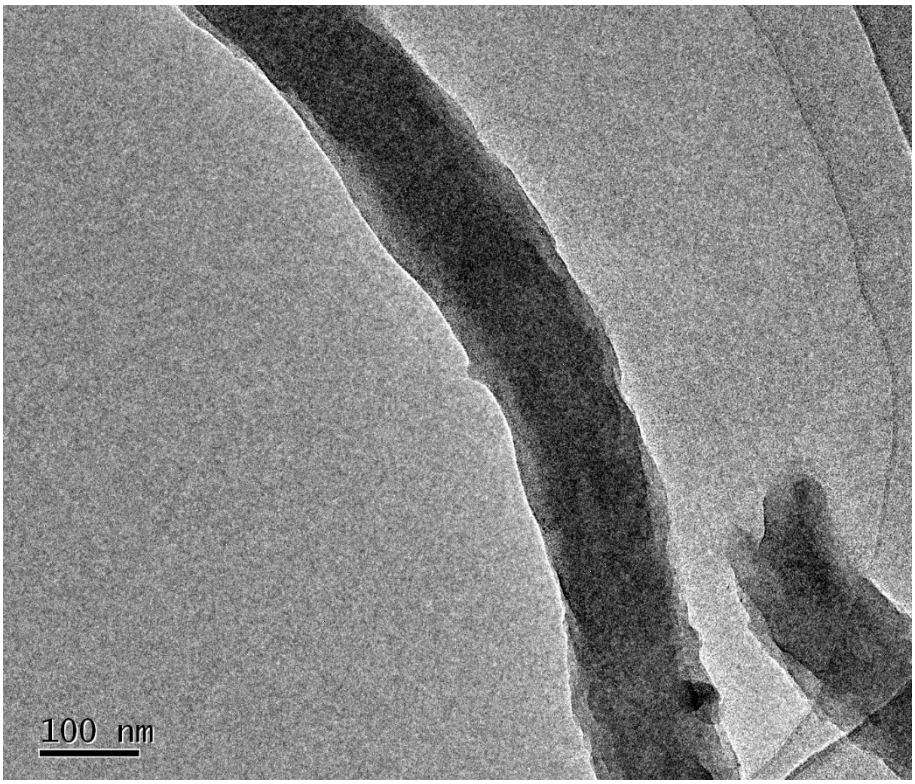

Figure S7. TEM image of sp^2c-COF_{dpy}-Ni.

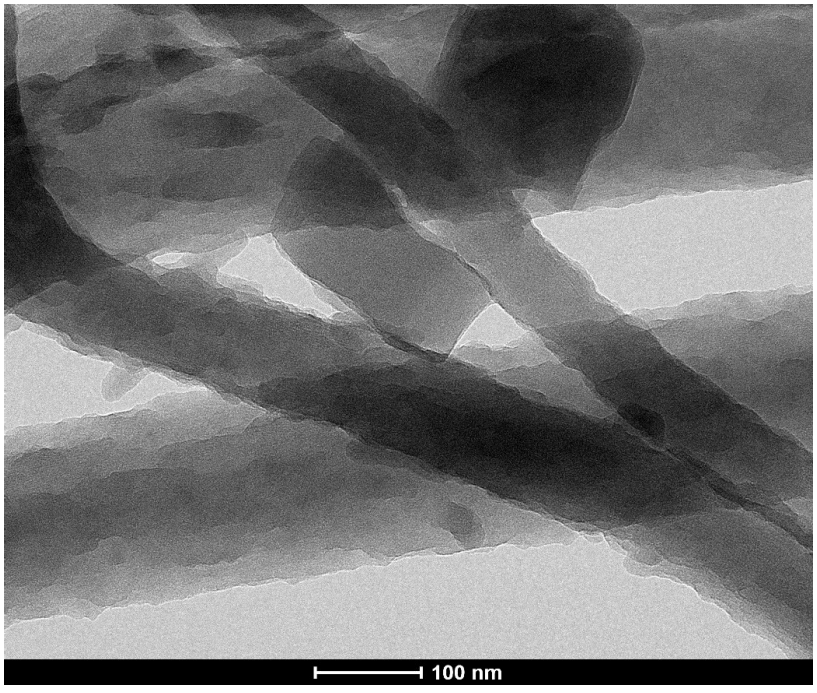

Figure S8. TEM image of sp^2c-COF_{dpy}-Ni.

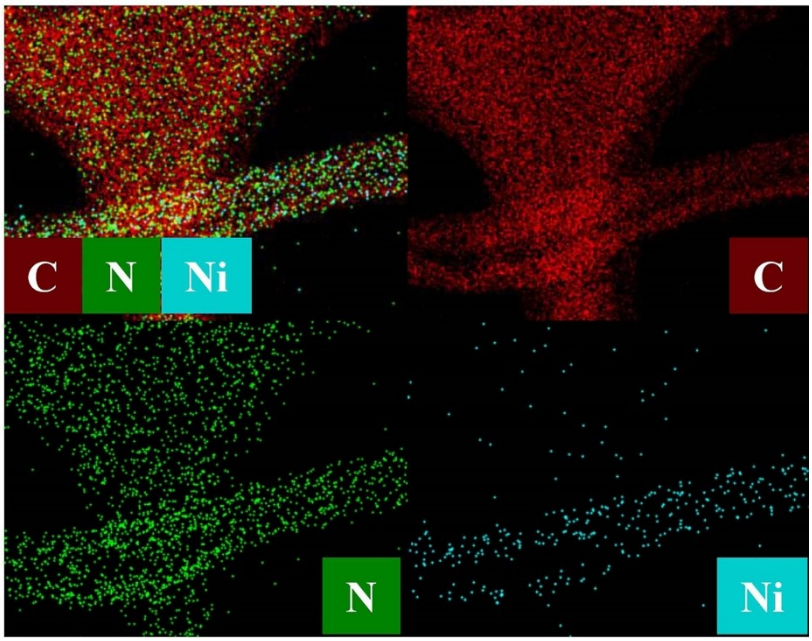

Figure S9. EDX elemental mapping images of $sp^2c\text{-}COF_{dpy}\text{-}Ni$.

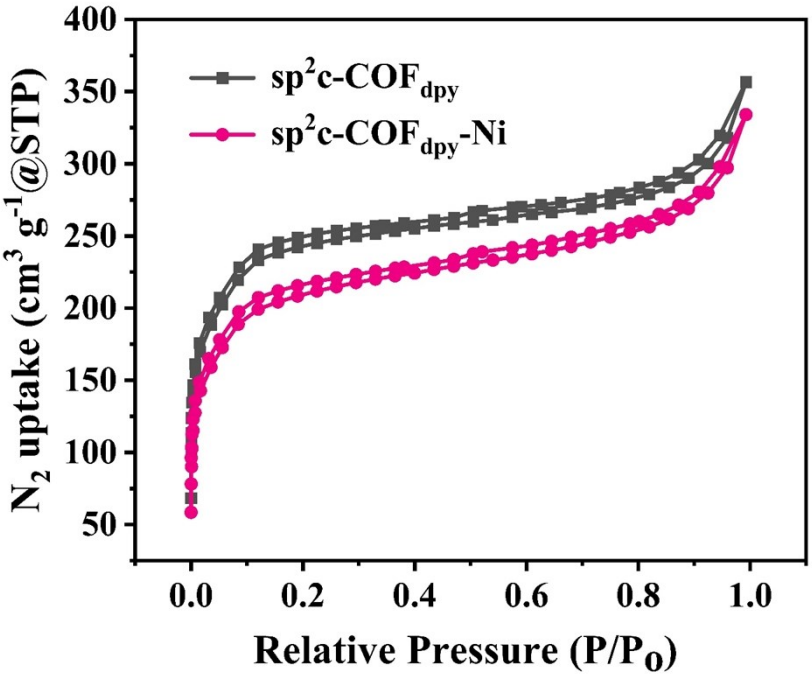

Figure S10. N_2 adsorption–desorption isotherm of $sp^2c\text{-}COF_{dpy}$ and $sp^2c\text{-}COF_{dpy}\text{-}Ni$.

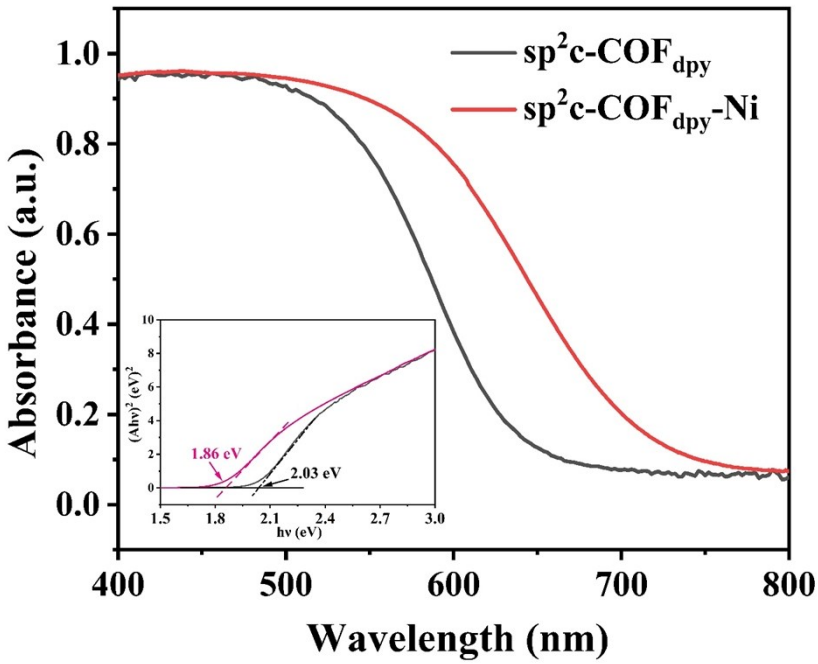

Figure S11. Solid-state UV/Vis DRS spectra of sp^2c-COF_{dpy} and sp^2c-COF_{dpy}-Ni. Inset shows the corresponding bandgap.

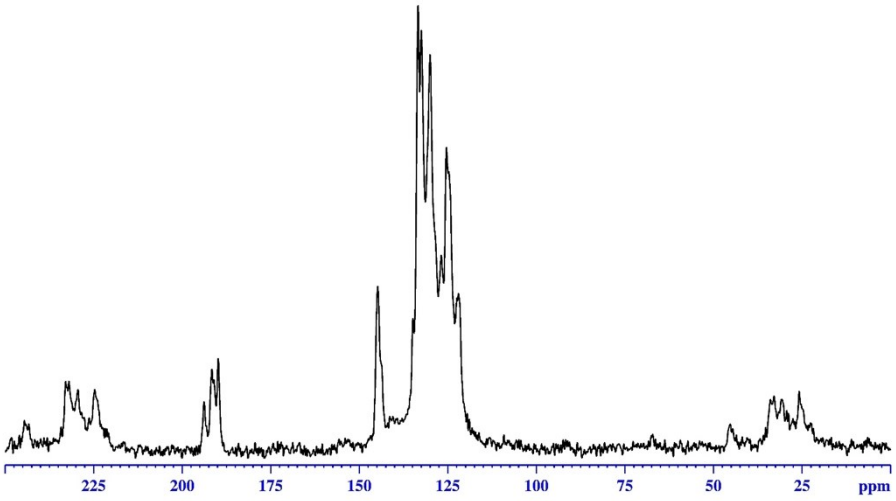

Figure S12. Solid-state ^{13}C CP/MAS NMR spectra of sp^2c-COF_{dpy}-Ni^{II}ArBr.

Table1 S1. EXAFS fitting parameters at the Ni K-edge various samples（S_0^2=0.80）

Sample	Path	C.N.	R (Å)	$\sigma^2\times10^3$ (Å^2)	ΔE (eV)	R factor
Ni foil	Ni-Ni	12*	2.48±0.01	5.9±0.2	6.5±0.4	0.001
sp^2c-COFdpy-Ni	Ni-O	6.8±0.6	2.06±0.01	8.2±1.0	-2.6±0.9	0.002

[a]*N*: coordination numbers; [b]*R*: bond distance; [c]σ^2: Debye-Waller factors; [d] ΔE_0: the inner potential correction. *R* factor: goodness of fit. * the experimental EXAFS fit of metal foil by fixing CN as the known crystallographic value.

4. Characterization of etherification production

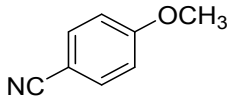

4-Methoxybenzonitrile (2): white solid, 67 mg, 99% yield. ^{1}H NMR (600 MHz, $CDCl_3$) δ (ppm) 7.59 (d, *J* = 8.8 Hz, 2H), 6.95 (d, *J* = 8.8 Hz, 2H), 3.86 (s, 3H); ^{13}C NMR (150 MHz, $CDCl_3$) δ (ppm) 162.8, 134.0, 119.2, 114.7, 103.9, 55.5. HRMS (ESI) m/z calcd. for C_8H_8NO [$(M+H)^+$] 134.0600, found 134.0590. Melting points: 61.1 °C.

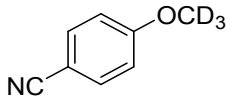

Deuterated 4-methoxybenzonitrile (2a): white solid, 67 mg, 99% yield. ^{1}H NMR (600 MHz, $CDCl_3$) δ (ppm) 7.57 (d, *J* = 9.0 Hz, 2H), 6.93 (d, *J* = 9.0 Hz, 2H); ^{13}C NMR (150 MHz, $CDCl_3$) δ (ppm) 162.8, 134.0, 119.2, 114.7, 103.8, 54.7 (m). HRMS (ESI) m/z calcd. for $C_8H_5D_3NO$ [$(M+H)^+$] 137.0789, found 137.0795. Melting points: 61.5 °C.

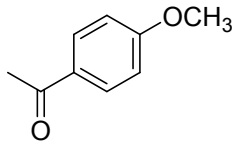

4-Acetanisole (3): colorless oil, 74 mg, 98% yield. ^{1}H NMR (600 MHz, $CDCl_3$) δ (ppm) 7.93 (d, *J* = 8.8 Hz, 2H), 6.92 (d, *J* = 8.8 Hz, 2H), 3.86 (s, 3H), 2.55 (s, 3H); ^{13}C NMR (150 MHz, $CDCl_3$) δ (ppm) 196.8, 163.3, 130.5, 130.3, 113.6, 55.4, 26.3. HRMS (ESI) m/z calcd. for $C_9H_{11}O_2$ [$(M+H)^+$] 151.0754, found 151.0758.

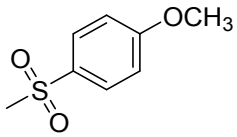

4-Methylsulfonylanisole (4): white solid, 92 mg, 98% yield. ^{1}H NMR (600 MHz, $CDCl_3$) δ (ppm) 7.87 (d, *J* = 8.9 Hz, 2H), 7.02 (d, *J* = 8.9 Hz, 2H), 3.89 (s, 3H), 3.03 (s, 3H); ^{13}C NMR (150 MHz, $CDCl_3$) δ (ppm) 163.6, 132.1, 129.5, 114.5, 55.7, 44.8. HRMS (ESI) m/z calcd. for $C_8H_{11}O_3S$ [$(M+H)^+$] 187.0423, found 187.0402. Melting points: 119-120 °C.

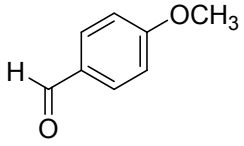

4-Methoxybenzaldehyde (5): colorless oil, 66 mg, 97% yield. ^{1}H NMR (600 MHz, $CDCl_3$) δ (ppm) 9.88 (s, 1H), 7.84 (d, *J* = 8.8 Hz, 2H), 7.00 (d, *J* = 8.9 Hz, 2H), 3.89 (s, 3H); ^{13}C NMR (150 MHz, $CDCl_3$) δ (ppm) 190.9, 164.5, 132.0, 129.8, 114.3, 55.6. HRMS (ESI) m/z calcd. for $C_8H_9O_2$ [$(M+H)^+$] 137.0597, found 137.0537.

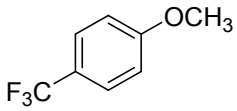

4-(Trifluoromethyl)anisole (**6**): colorless oil, 86 mg, 98% yield. ^{1}H NMR (600 MHz, $CDCl_3$) δ (ppm) 7.55 (d, *J* = 8.7 Hz, 2H), 6.96 (d, *J* = 8.7 Hz, 2H), 3.85 (s, 3H); ^{13}C NMR (150 MHz, $CDCl_3$) δ (ppm) 162.0, 126.9 (q, *J* = 8.7 Hz), 124.5 (q, *J* = 270.9 Hz), 122.8 (q, *J* = 32.7 Hz), 113.9, 55.4; ^{19}F NMR (376 Hz, $CDCl_3$) δ (ppm) -61.49. HRMS (ESI) m/z calcd. for $C_8H_8F_3O$ [$(M+H)^+$] 177.0522, found 177.0529. Data was consistent with that reported in the literature.[4]

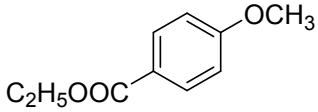

Ethyl *p*-anisate (**7**): colorless oil, 88 mg, 98% yield. ^{1}H NMR (600 MHz, $CDCl_3$) δ (ppm) 7.99 (d, *J* = 8.9 Hz, 2H), 6.90 (d, *J* = 8.9 Hz, 2H), 4.33 (q, *J* = 7.1 Hz, 2H), 3.84 (s, 3H), 1.37 (q, *J* = 7.1 Hz, 3H); ^{13}C NMR (150 MHz, $CDCl_3$) δ (ppm) 166.3, 163.2, 131.5, 122.9, 113.5, 60.6, 55.3, 14.3. HRMS (ESI) m/z calcd. for $C_{10}H_{13}O_3$ [$(M+H)^+$] 181.0859, found 181.0865.

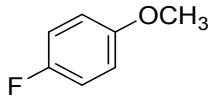

4-Fluoroanisole (8): colorless oil, 62 mg, 99% yield. ^{1}H NMR (600 MHz, $CDCl_3$) δ (ppm) 7.01–6.95 (m, 2H), 6.86– 6.81 (m, 2H), 3.78 (s, 3H); ^{13}C NMR (150 MHz, $CDCl_3$) δ (ppm) 157.2 (d, *J* = 237.8 Hz), 155.7 (d, *J* = 1.9 Hz), 115.7 (d, *J* = 23.1 Hz), 114.7 (d, *J* = 7.9 Hz), 55.7. ^{19}F NMR (376 Hz, $CDCl_3$) δ (ppm) -124.4. HRMS (ESI) m/z calcd. for C_7H_8FO [$(M+H)^+$] 127.0554, found 127.0560.

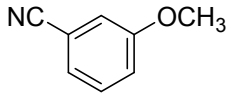

3-Methoxybenzonitrile (9): white solid, 64 mg, 96% yield. ^{1}H NMR (600 MHz, $CDCl_3$) δ (ppm) 7.39-7.33 (m, 1H), 7.24-7.21 (m, 1H), 7.15-7.10 (m, 2H), 3.82 (s, 3H);

^{13}C NMR (150 MHz, $CDCl_3$) δ (ppm) 159.6, 130.3, 124.4, 119.2, 118.7, 116.8, 113.1, 55.5. HRMS (ESI) m/z calcd. for C_8H_8NO [$(M+H)^+$] 134.0600, found 134.0608. Melting points: 163.5 °C.

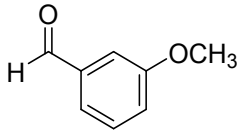

3-Methoxybenzaldehyde (10): white solid, 67 mg, 98% yield. ^{1}H NMR (600 MHz, $CDCl_3$) δ (ppm) 9.98 (s, 1H), 7.47-7.43 (m, 2H), 7.39 (d, *J* = 1.9 Hz, 1H), 7.18 (dt, *J* = 7.1, 2.4 Hz, 1H), 3.87 (s, 3H); ^{13}C NMR (150 MHz, $CDCl_3$) δ (ppm) 192.1, 160.1, 137.8, 130.0, 123.5, 121.5, 112.0, 55.4. HRMS (ESI) m/z calcd. for $C_8H_9O_2$ [$(M+H)^+$] 137.0597, found 137.0604. Melting points: 186.3 °C.

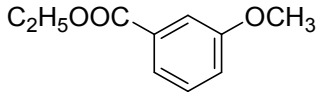

Ethyl *m*-anisate (**11**): colorless oil, 87 mg, 97% yield. ^{1}H NMR (600 MHz, $CDCl_3$) δ (ppm) 7.63 (d, *J* = 7.6 Hz, 1H), 7.56 (s, 1H), 7.33 (t, *J* = 7.9 Hz, 1H), 7.09 (dd, *J* = 6.2 , 2.6 Hz, 1H), 4.37 (q, *J* = 7.1 Hz, 2H)，3.84 (s, 3H), 1.39 (t, *J* = 7.1 Hz, 3 H); ^{13}C NMR (150 MHz, $CDCl_3$) δ (ppm) 166.4, 159.5, 131.8, 129.3, 121.9, 119.2, 113.9, 61.0, 55.4, 14.3. HRMS (ESI) m/z calcd. for $C_{10}H_{13}O_3$ [$(M+H)^+$] 181.0859, found 181.0864.

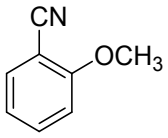

2-Methoxybenzonitrile (12): colorless oil, 62 mg, 93% yield. ^{1}H NMR (600 MHz, $CDCl_3$) δ (ppm) 7.57-7.49 (m, 2H), 7.03-6.95 (m, 2H), 3.92 (s, 3H); ^{13}C NMR (150 MHz, $CDCl_3$) δ (ppm) 161.2, 134.3, 133.7, 120.7, 116.4, 111.2, 101.7, 55.9. HRMS (ESI) m/z calcd. for C_8H_8NO [$(M+H)^+$] 134.0600, found 134.0609.

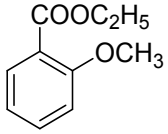

Ethyl *o*-anisate (**13**): colorless oil, 54 mg, 99% yield. ^{1}H NMR (600 MHz, $CDCl_3$) δ (ppm) 7.78 (dd, *J* = 7.8, 1.7 Hz, 1H), 7.45 (dt, *J* = 7.8, 1.7 Hz, 1H), 7.00-6.95 (m, 2H), 4.35 (q, *J* = 7.1 Hz, 2H), 3.90 (s, 3H), 1.37 (t, *J* = 7.1 Hz, 3H); ^{13}C NMR (150 MHz,

$CDCl_3$) δ (ppm) 166.2, 159.1, 133.3, 131.4, 120.4, 120.1, 112.0, 60.7, 55.9, 14.3. HRMS (ESI) m/z calcd. for $C_{10}H_{13}O_3$ [$(M+H)^+$] 181.0859, found 181.0866.

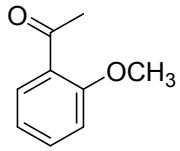

2-Acetanisole (14): colorless oil, 65 mg, 87% yield. ^1H NMR (600 MHz, $CDCl_3$) δ (ppm) 7.72 (dd, *J* = 7.7, 1.8 Hz, 1H), 7.47-7.43 (m, 1H), 7.00-6.95 (m, 2H), 3.90 (s, 3H), 2.60 (s, 3H); ^{13}C NMR (150 MHz, $CDCl_3$) δ (ppm) 199.8, 158.9, 133.6, 130.3, 128.2, 120.5, 111.5, 55.4, 31.8. HRMS (ESI) m/z calcd. for $C_9H_{11}O_2$ [$(M+H)^+$] 151.0754, found 151.0761.

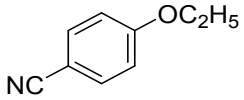

4-Ethoxybenzonitrile (15): white solid, 71 mg, 97% yield. ^1H NMR (600 MHz, $CDCl_3$) δ (ppm) 7.55 (d, *J* = 8.9 Hz, 2H), 6.91 (d, *J* = 8.8 Hz, 2H), 4.06 (q, *J* = 7.0 Hz, 2H), 1.42 (t, *J* = 7.0 Hz, 2H); ^{13}C NMR (150 MHz, $CDCl_3$) δ (ppm) 162.2, 133.9, 119.2, 115.1, 103.6, 63.8, 14.4. HRMS (ESI) m/z calcd. for $C_9H_{10}NO$ [$(M+H)^+$] 148.0757, found 148.0765. Melting points: 60.8 °C.

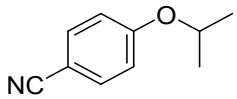

4-isopropoxybenzonitrile (16): white solid, 78 mg, 97% yield. ^1H NMR (600 MHz, $CDCl_3$) δ (ppm) 7.56 (d, *J* = 8.9 Hz, 2H), 6.90 (d, *J* = 8.8 Hz, 2H), 4.60 (hept, *J* = 6.1 Hz, 1H), 1.35 (d, *J* = 6.1 Hz, 6H); ^{13}C NMR (150 MHz, $CDCl_3$) δ (ppm) 161.3, 134.0, 119.3, 116.0, 103.3, 70.4, 21.8. HRMS (ESI) m/z calcd. for $C_{10}H_{12}NO$ [$(M+H)^+$] 162.0913, found 162.0919. Melting points: 51.9 °C.

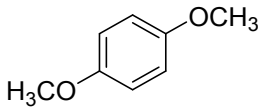

1,4-Dimethoxybenzene (17): colorless oil, 68 mg, 98% yield. ^1H NMR (600 MHz, $CDCl_3$) δ (ppm) 6.85 (s, 4H), 3.77 (s, 6H); ^{13}C NMR (150 MHz, $CDCl_3$) δ (ppm) 133.7, 114.6, 55.7. HRMS (ESI) m/z calcd. for $C_8H_{11}O_2$ [$(M+H)^+$] 139.0754, found 139.0761.

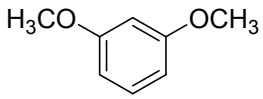

1,3-Dimethoxybenzene (18): colorless oil, 68 mg, 98% yield. ^{1}H NMR (600 MHz, $CDCl_3$) δ (ppm) 7.19 (t, *J* = 8.2 Hz, 1H), 6.52 (dd, *J* = 8.2, 2.4 Hz, 2H), 6.47 (t, *J* = 2.4 Hz, 1H), 3.80 (s, 6H); ^{13}C NMR (150 MHz, $CDCl_3$) δ (ppm) 160.8, 129.9, 106.1, 100.4, 55.2. HRMS (ESI) m/z calcd. for $C_8H_{11}O_2$ [$(M+H)^+$] 139.0754, found 139.0760.

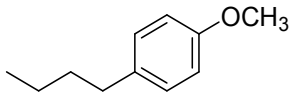

4-Butylanisol (19): colorless oil, 70 mg, 85% yield. ^{1}H NMR (600 MHz, $CDCl_3$) δ (ppm) 7.11 (d, *J* = 8.6 Hz, 2H), 6.84 (d, *J* = 8.6 Hz, 2H), 3.80 (s, 3H), 2.57 (t, *J* = 7.7 Hz, 2H), 1.65-1.54 (m, 2H), 1.41-1.32 (m, 2H), 0.94 (t, *J* = 7.4 Hz, 3H); ^{13}C NMR (150 MHz, $CDCl_3$) δ (ppm) 157.6, 134.0, 129.2, 113.6, 55.2, 34.7, 33.9, 22.3, 13.9. HRMS (ESI) m/z calcd. for $C_{11}H_{17}O$ [$(M+H)^+$] 165.1274, found 165.1283.

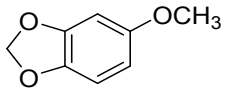

5-Methoxy-1,3-benzodioxole (20): colorless oil, 75 mg, 99% yield. ^{1}H NMR (600 MHz, $CDCl_3$) δ (ppm) 6.71 (d, *J* = 8.5 Hz, 1H), 6.49 (d, *J* = 2.5 Hz, 1H), 6.31 (dd, *J* = 8.5, 2.5 Hz, 1H), 5.91 (s, 2H), 3.75 (s, 3H); ^{13}C NMR (150 MHz, $CDCl_3$) δ (ppm) 155.2, 148.3, 141.6, 107.9, 104.7, 101.1, 97.5, 56.0. HRMS (ESI) m/z calcd. for $C_8H_9O_3$ [$(M+H)^+$] 153.0546, found 153.0550.

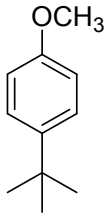

***p-tert*-Butylanisole (21)**: colorless oil, 80 mg, 98% yield. ^{1}H NMR (600 MHz, $CDCl_3$) δ (ppm) 7.33 (d, *J* = 8.9 Hz, 2H), 6.87 (d, *J* = 8.9 Hz, 2H), 3.81 (s, 3H), 1.32 (s, 9H); ^{13}C NMR (150 MHz, $CDCl_3$) δ (ppm) 157.3, 143.3, 126.2, 113.3, 55.2, 34.0, 31.5. HRMS (ESI) m/z calcd. for $C_{11}H_{17}O$ [$(M+H)^+$] 165.1274, found 165.1282.

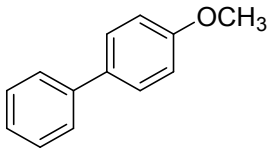

4-Methoxybiphenyl (22): white solid, 89 mg, 97% yield. ^{1}H NMR (600 MHz, $CDCl_3$) δ (ppm) 7.63-7.54 (m, 4H), 7.46 (t, *J* = 7.8 Hz, 2H), 7.37-7.32 (m, 1H), 7.02 (d, *J* = 8.8 Hz, 2H), 3.88 (s, 3H); ^{13}C NMR (150 MHz, $CDCl_3$) δ (ppm) 159.1, 140.8, 133.7, 128.7, 128.1, 126.7, 126.6, 114.1, 55.2. HRMS (ESI) m/z calcd. for $C_{13}H_{13}O$ [$(M+H)^+$] 185.0961, found 185.0958. Melting points: 88.7 °C.

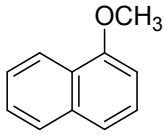

1-Methoxynaphthalene (23): colorless oil, 51 mg, 64% yield. ^{1}H NMR (600 MHz, $CDCl_3$) δ (ppm) 8.27 (d, *J* = 7.6 Hz, 1H), 7.80 (d, *J* = 8.2 Hz, 1H), 7.53-7.37 (m, 4H), 6.83 (d, *J* = 7.6 Hz, 1H), 4.02 (s, 3H); ^{13}C NMR (150 MHz, $CDCl_3$) δ (ppm) 155.4, 134.4, 127.4, 126.4, 125.9, 125.6, 125.1, 121.9, 120.2, 103.7, 55.5. HRMS (ESI) m/z calcd. for $C_{11}H_{11}O$ [$(M+H)^+$] 159.0804, found 159.0814.

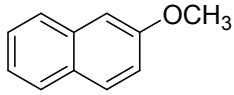

2-Methoxynaphthalene (24): white solid, 77 mg, 98% yield. ^{1}H NMR (600 MHz, $CDCl_3$) δ (ppm) 7.80 (d, *J* = 8.1 Hz, 1H), 7.77 (d, *J* = 8.6 Hz, 2H), 7.51-7.45 (m, 1H), 7.41-7.35 (m, 1H), 7.19 (dd, *J* = 8.8, 2.5 Hz, 1H), 7.17 (d, *J* = 2.5 Hz, 1H), 3.95 (s, 3H); ^{13}C NMR (150 MHz, $CDCl_3$) δ (ppm) 157.6, 134.5, 129.3, 128.9, 127.6, 126.7, 126.3, 123.5, 118.7, 105.7, 55.2. HRMS (ESI) m/z calcd. for $C_{11}H_{11}O$ [$(M+H)^+$] 159.0804, found 159.0812. Melting points: 72.5 °C.

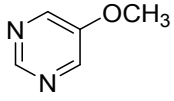

5-Methoxypyrimidine (25): white solid, 53 mg, 96% yield. ^{1}H NMR (600 MHz, $CDCl_3$) δ (ppm) 8.85 (s, 1H), 8.41 (s, 2H), 3.92 (s, 3H); ^{13}C NMR (150 MHz, $CDCl_3$) δ (ppm) 153.5, 151.5, 143.1, 55.8. HRMS (ESI) m/z calcd. for $C_5H_7N_2O$ [$(M+H)^+$] 111.0553, found 111.0559. Melting points: 46.7 °C.

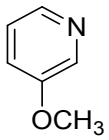

3-Methoxypyridine (26): colorless oil, 30 mg, 55% yield. ^{1}H NMR (600 MHz, $CDCl_3$) δ (ppm) 8.30 (s, 1H), 8.20 (d, J = 2.0 Hz, 1H), 7.22-7.14 (m, 1H), 3.92 (s, 3H); ^{13}C NMR (150 MHz, $CDCl_3$) δ (ppm) 155.6, 142.0, 137.5, 123.7, 120.3, 55.4. HRMS (ESI) m/z calcd. for C_6H_8NO [$(M+H)^+$] 110.0600, found 110.0608.

5. Computational Details

Density functional theory (DFT) calculations were performed for the theoretical investigation of sp^2c-COF_{dpy}-Ni catalyzed methoxylation reaction. The DFT method employed in this work is M062x with well documented performance on transition metal and reaction barrier height.[5] The polymer was truncated to one unit, as shown in Figure 3. Geometries were determined with 6-31G(d) basis set while energies were determined by single point calculations with 6-311+G(d,p) basis set upon optimized structures. All calculations were performed using the Gaussian09 package.[6] Local minima and transition state structures were obtained by geometry optimization. Especially, the transition states were located employing the TS keyword in Gaussian09, which means optimization to a transition state using the Berny algorithm. Frequency analysis was used to verify the nature of stationary points. Reactant, product and intermediates have zero negative frequency while transition states have only one negative frequency.

6. Theoretically optimized structures

Figure. S13 sp^2c-COF_{dpy}-Ni -Cl model

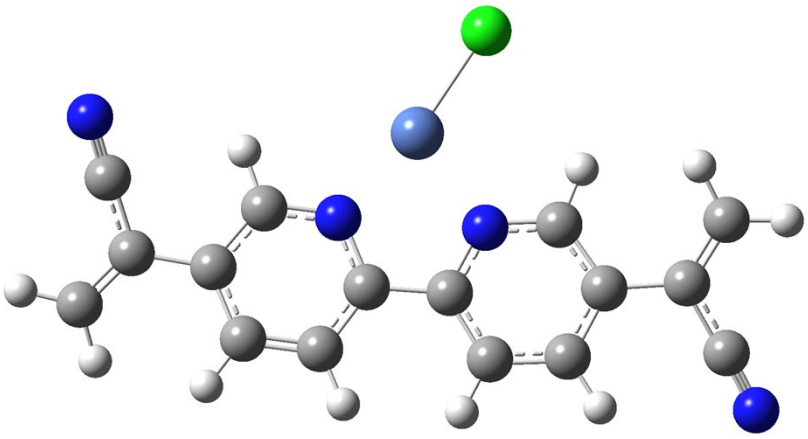

Corresponding Coordinates:

C	5.72232800	-1.50118000	-0.12438800
C	4.86732800	-0.36370800	0.12347300
C	5.42832000	0.82672000	0.37544400
C	2.48609800	0.41764900	-0.00734500
C	0.67980300	-1.03389200	0.06504900
C	1.52507600	-2.13771800	0.14959400
C	3.41011100	-0.62920000	0.09503700
C	2.89906200	-1.92726800	0.16207700
C	-5.04212300	-0.98606900	-0.09445900
C	-5.84132800	-1.97797800	-0.50768600
C	-1.50888000	-2.30995200	0.09904700
C	-2.89413100	-2.29011800	0.06879800
C	-0.80562500	-1.10651800	0.04176800
C	-3.56488700	-1.06998400	-0.02765700
C	-2.78296700	0.08846800	-0.06148400
N	1.17769900	0.20728100	-0.01351200
N	6.37181300	-2.43891800	-0.31667700
N	-1.45145200	0.07352800	-0.03334300
H	2.77671800	1.46221600	-0.10098100
H	1.13660000	-3.14754000	0.20547700
H	3.57691400	-2.77385800	0.22404400
H	4.83116600	1.70398000	0.59936200
H	-3.44963800	-3.21991900	0.14142900
H	-3.24849200	1.06923000	-0.11646600
H	-5.43617800	-2.92346400	-0.85204200
H	-0.98515000	-3.25486100	0.17891800
Ni	-0.21689800	1.75375700	-0.10443100

Cl	0.79755200	3.72785300	-0.17032500
H	-6.91785900	-1.85610200	-0.52635500
H	6.50579300	0.94287200	0.37065000
C	-5.63561700	0.27023800	0.29953200
N	-6.08813400	1.28694100	0.61421200

Figure S14 Transition state TS1, R=H

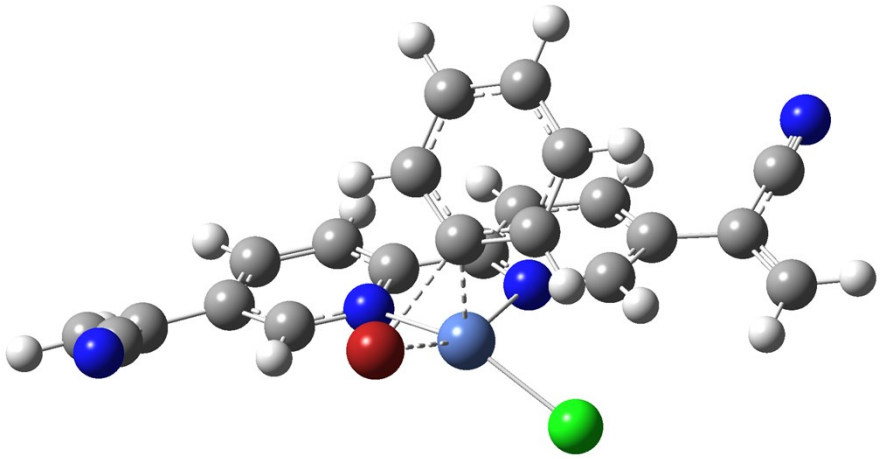

Corresponding Coordinates:

C	6.00934400	1.75416100	0.19652500
C	5.06053700	0.93365200	-0.51860700
C	5.50756600	-0.03062100	-1.33477600
C	2.63714600	0.32290800	-0.60862000
C	0.94012600	1.79353100	-0.04192500
C	1.86332800	2.77411200	0.31403000
C	3.63139100	1.25985600	-0.30895200
C	3.21910200	2.49892400	0.18218700
C	-4.76642500	2.22348100	-0.05565100
C	-5.47732100	3.34552200	-0.22668000
C	-1.13691400	3.18170600	0.37986100
C	-2.51985100	3.27368700	0.37751500
C	-0.53396700	1.97894600	0.01128800
C	-3.28715600	2.17120200	-0.00164100
C	-2.60304700	0.99748500	-0.33404300
N	1.34608700	0.59420900	-0.48043400
N	6.73305400	2.44439200	0.77798100
N	-1.27481600	0.91058400	-0.33065100
H	2.85608800	-0.67807000	-0.97172900
H	1.54483100	3.74055100	0.68534800
H	3.95722700	3.24883200	0.45345500
H	4.82693400	-0.63926500	-1.92197500

H	-3.00043700	4.19648900	0.68801000
H	-3.13628900	0.08872700	-0.60541000
H	-4.99195300	4.30590100	-0.36444400
H	-0.54034700	4.03718700	0.67164400
Ni	-0.13723300	-0.87712400	-0.84956500
Cl	1.16062400	-1.98443600	-2.42123700
H	-6.56035000	3.32151900	-0.25093100
H	6.56981500	-0.21845700	-1.44036800
C	-5.46424100	0.96519700	0.06729500
N	-6.00737400	-0.05101300	0.16514100
C	1.72029800	-2.80615800	2.19612700
C	1.40187200	-2.02535800	3.30620700
C	0.30670800	-1.16379900	3.26243300
C	-0.46828900	-1.06896500	2.10818100
C	-0.09852200	-1.82336800	0.99898200
C	0.95730400	-2.72961000	1.03093100
H	2.56399000	-3.48885000	2.23364800
H	1.99568900	-2.10051100	4.21148900
H	0.04310300	-0.57091100	4.13337900
H	-1.34048300	-0.42362400	2.07449800
H	1.19166800	-3.32584900	0.15474000
Br	-1.96686100	-2.49842700	-0.33516500

Figure S15 Intermediate state Int1, R=H

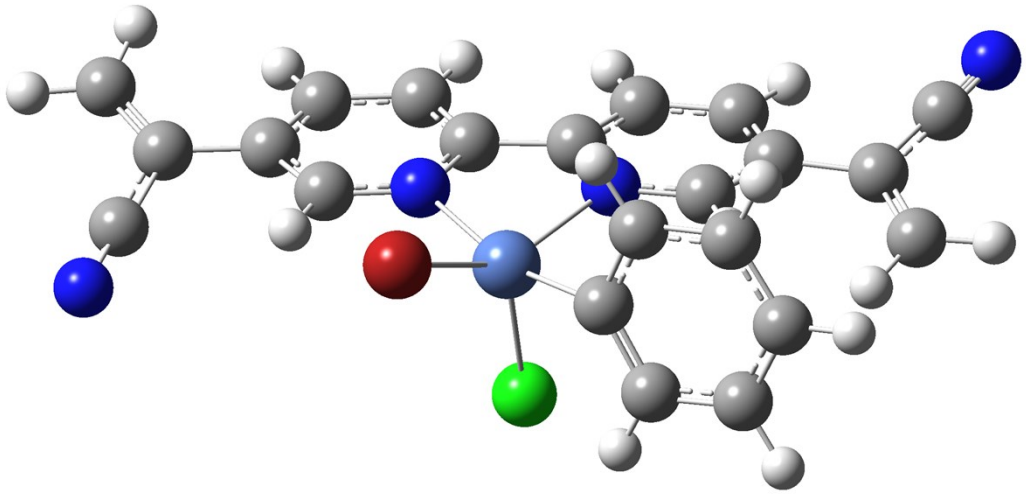

Corresponding Coordinates:

C	-5.36476600	2.95359600	-0.35147700
C	-4.61017300	1.77356700	-0.00070900
C	-5.26408300	0.67060100	0.38839600
C	-2.33001000	0.75832300	-0.13847600

C	-0.37988500	2.00690700	-0.16096200
C	-1.10901500	3.19318600	-0.13604600
C	-3.13672800	1.89750000	-0.08175400
C	-2.49610000	3.13608800	-0.10094500
C	5.31086300	1.42162800	-0.16557800
C	6.20205400	2.29390800	-0.65368100
C	1.91597900	3.08521800	-0.20632600
C	3.29303100	2.92534800	-0.19030400
C	1.10469500	1.95283200	-0.16148700
C	3.84686100	1.64507700	-0.14598000
C	2.96104800	0.56394100	-0.09042500
N	-1.00573300	0.81756400	-0.17866300
N	-5.93320300	3.92109400	-0.63211400
N	1.64231200	0.72536200	-0.10380300
H	-2.76036400	-0.23814000	-0.16372500
H	-0.61061200	4.15469600	-0.12853000
H	-3.08030100	4.05167300	-0.07797800
H	-4.73545500	-0.22714000	0.69480800
H	3.93494100	3.80052200	-0.19225900
H	3.31324800	-0.46502300	-0.04018800
H	5.88959500	3.23392500	-1.09592400
H	1.48899900	4.07982800	-0.24164200
Ni	0.25600500	-0.83919800	0.18661500
Cl	0.12831800	-0.42259600	2.46515500
H	7.26318300	2.07546600	-0.63536100
H	-6.34733100	0.65188200	0.41861500
C	5.78840400	0.16310400	0.35743000
N	6.16755200	-0.84776000	0.77147000
C	-3.28462900	-3.02698600	0.99622400
C	-3.88626800	-3.08864100	-0.26082500
C	-3.15742400	-2.77268900	-1.40664900
C	-1.82021400	-2.37926500	-1.29993300
C	-1.27945000	-2.27350400	-0.02766700
C	-1.95043200	-2.62699700	1.13017300
H	-3.84931400	-3.29131200	1.88563800
H	-4.92046300	-3.40747700	-0.34952300
H	-3.61646300	-2.84953200	-2.38780400
H	-1.23253600	-2.15299900	-2.18383600
H	-1.47679500	-2.54044600	2.10194400
Br	1.51917400	-2.68984400	-0.78552300

Figure S16 Transition state TS2, R=H

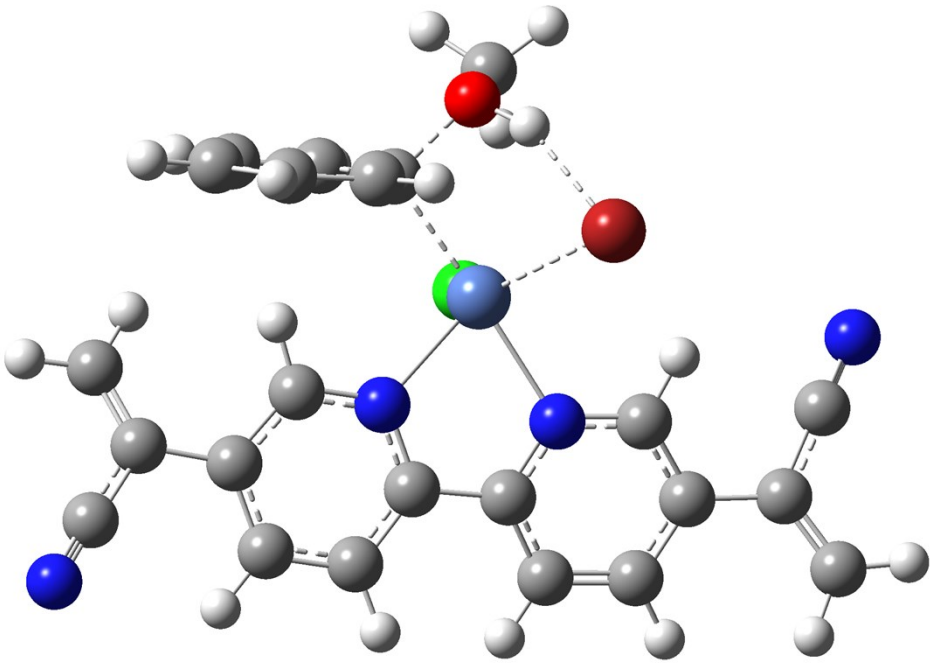

Corresponding Coordinates:

C	-5.47287300	2.99958800	-0.51702000
C	-4.71826800	1.88613500	0.00827000
C	-5.36869600	0.83496100	0.52343800
C	-2.41606200	0.89307900	-0.04659200
C	-0.49489000	2.18058100	-0.02430700
C	-1.24645700	3.35352900	-0.05210900
C	-3.24436500	2.02112800	-0.03155500
C	-2.63033800	3.27197300	-0.06181000
C	5.20574400	1.82449400	0.06570100
C	6.08078700	2.80826400	-0.17959700
C	1.74642300	3.33545900	0.22535800
C	3.12762800	3.23098100	0.25836400
C	0.98931500	2.18319800	0.00958600
C	3.73413300	1.98877700	0.06458500
C	2.89547100	0.88633200	-0.12591300
N	-1.08945200	0.97381400	-0.04473900
N	-6.04346100	3.91686900	-0.93094500
N	1.57162800	0.99151600	-0.15485900
H	-2.83340100	-0.10836800	-0.08331000
H	-0.76270300	4.32197300	-0.07918700
H	-3.23402300	4.17477800	-0.09017700
H	-4.82566400	0.00507500	0.96299900
H	3.72898200	4.11086100	0.46479200
H	3.29568900	-0.11567500	-0.26426800

H	5.74905000	3.81143300	-0.42487700
H	1.27364600	4.29426700	0.39921700
Ni	0.23238400	-0.72198000	0.06355000
Cl	0.62013000	-0.60867300	2.36537400
H	7.14827200	2.62407100	-0.15573300
H	-6.45195100	0.79329400	0.52034500
C	5.71551500	0.49921800	0.33231100
N	6.12019000	-0.56377200	0.54070200
C	-3.44155800	-2.32591400	1.14132500
C	-4.03883800	-2.34561700	-0.12751300
C	-3.22209800	-2.37935700	-1.26274100
C	-1.84111300	-2.43815700	-1.14755300
C	-1.23014500	-2.38852300	0.13949000
C	-2.06538200	-2.35786300	1.29239300
H	-4.06347100	-2.28386200	2.03240300
H	-5.11923700	-2.34603900	-0.22876900
H	-3.66779300	-2.38546900	-2.25336900
H	-1.21332000	-2.51562800	-2.03099800
H	-1.61441800	-2.30020000	2.27789100
Br	1.70290600	-2.00969000	-1.64814700
C	0.42069700	-3.96228500	1.51402500
H	0.81652100	-3.07300700	2.00936400
H	-0.38989900	-4.40937800	2.08717700
H	1.19829500	-4.70045400	1.31762500
O	-0.13791900	-3.61113000	0.22264200
H	0.59794500	-3.33545200	-0.40781400

7. References

1 M. G. Rabbani, A. K. Sekizkardes, O. M. El-Kadri, B. R. Kaafarani, H. M. El-Kaderi, *J. Mater. Chem.*, 2012, **22**, 25409-25417.

2 L.-Y. Liao, X.-R. Kong, X.-F. Duan, *J. Org. Chem.*, 2014, **79**, 777-782.

3 E. Jin, J. Li, K. Geng, Q. Jiang, H. Xu, Q. Xu, D. Jiang, *Nat. Commun.*, 2018, **9**, 4143.

4 T. Knauber, F. Arikan, G.-V. Röschenthaler, L. J. Gooßen, *Chem. Eur. J.*, 2011, **17**, 2689-2697.

5 Y. Zhao, D. G. Truhlar, *Theor. Chem. Acc.*, 2008, **120**, 215-241.

6 G. W. T. M. J. Frisch, H. B. Schlegel, G. E. Scuseria,M. A. Robb, J. R. Cheeseman, G. Scalmani, V. Barone, B. Mennucci,G. A. Petersson, H. Nakatsuji, M. Caricato, X. Li, H. P. Hratchian,A. F. Izmaylov, J. Bloino, G. Zheng, J. L. Sonnenberg, M. Hada,M. Ehara, K. Toyota, R. Fukuda, J. Hasegawa, M. Ishida, T. Nakajima,Y. Honda, O. Kitao, H. Nakai, T. Vreven, J. A. Montgomery, Jr.,J. E. Peralta, F. Ogliaro, M. Bearpark, J. J. Heyd, E. Brothers,K. N. Kudin, V. N. Staroverov, T. Keith, R. Kobayashi, J. Normand,K. Raghavachari, A. Rendell, J. C. Burant, S. S. Iyengar, J. Tomasi,M. Cossi, N. Rega, J. M. Millam, M. Klene, J. E. Knox, J. B. Cross,V. Bakken, C. Adamo, J. Jaramillo, R. Gomperts, R. E. Stratmann,O. Yazyev, A. J. Austin, R. Cammi, C. Pomelli, J. W. Ochterski,R. L. Martin, K. Morokuma, V. G. Zakrzewski, G. A. Voth,P. Salvador, J. J. Dannenberg, S. Dapprich, A. D. Daniels,O. Farkas, J. B. Foresman, J. V. Ortiz, J. Cioslowski,and D. J. Fox, *Gaussian 09, Revision D.01,Gaussian, Inc., Wallingford CT*, 2013.

8. Copies of ^{1}H NMR, ^{13}C NMR, ^{19}F NMR spectra

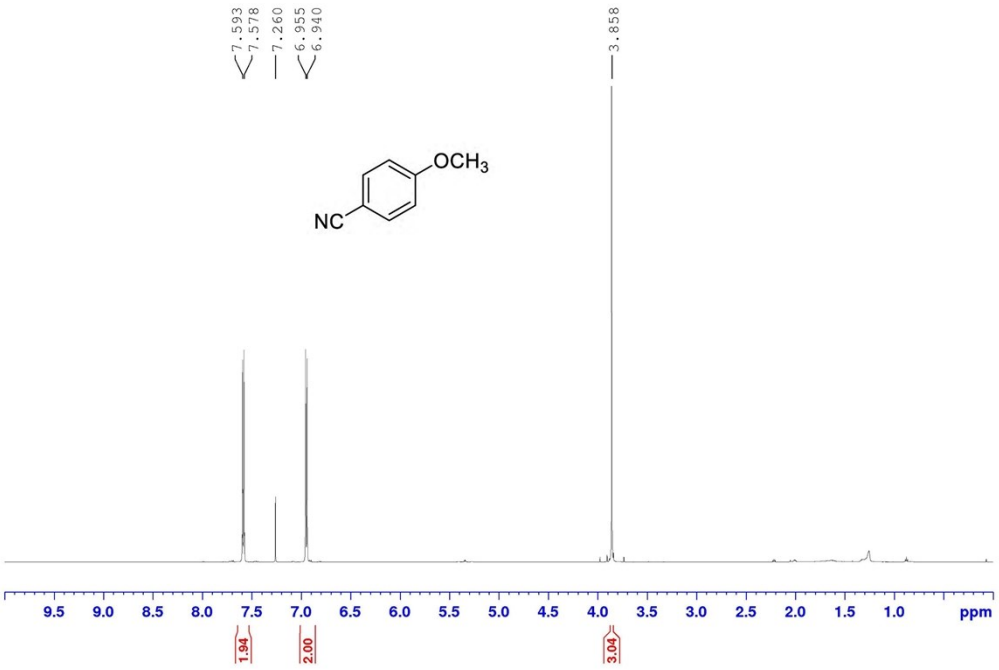

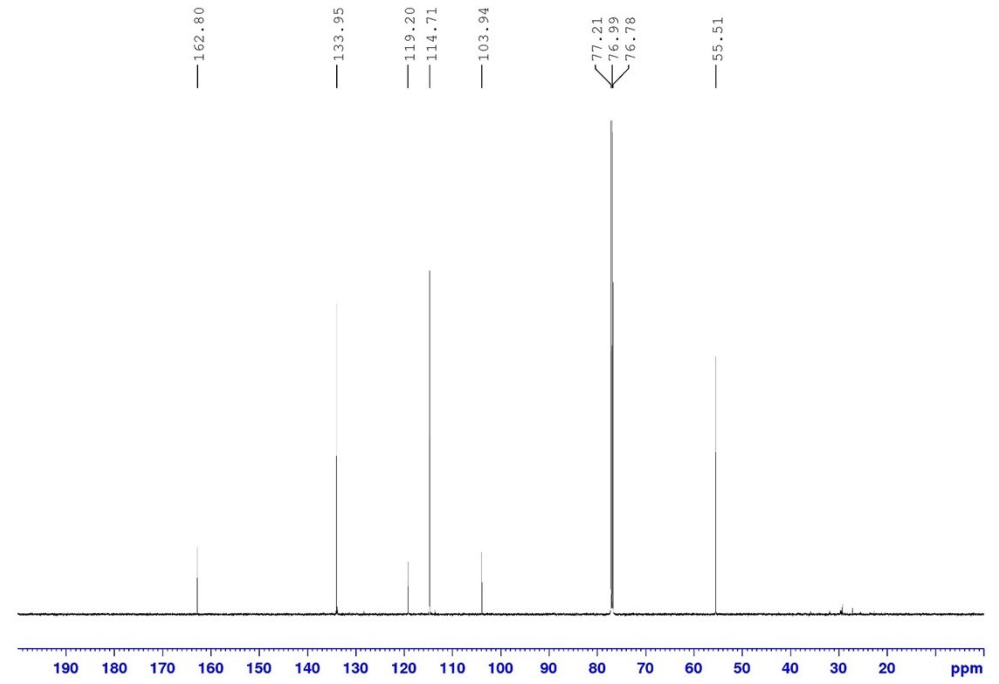

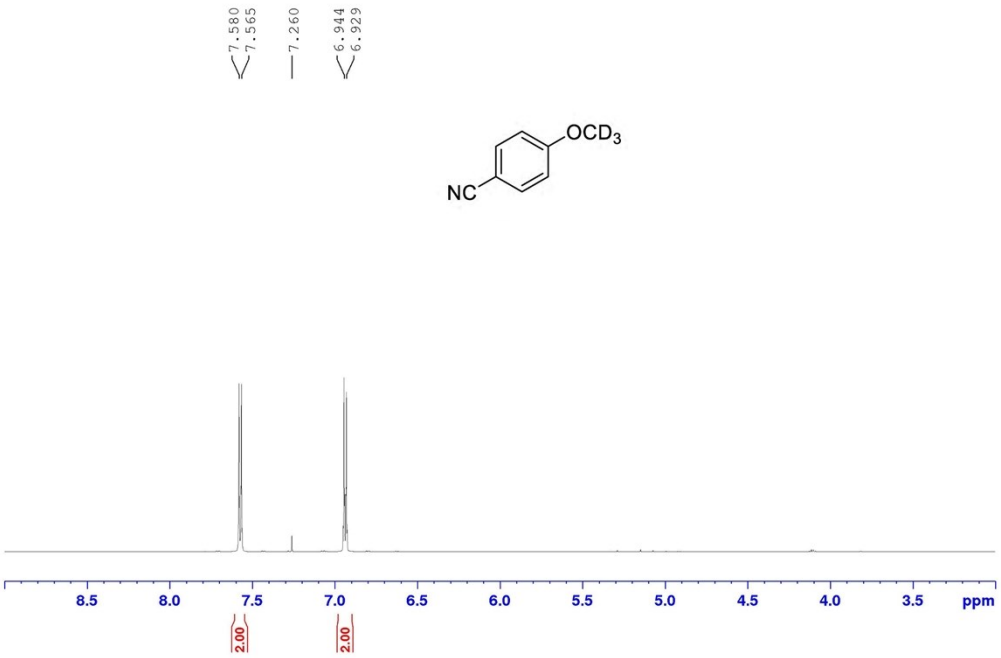
7.580
7.565
7.260
6.944
6.929
OCD3
NC
8.5
8.0
7.5
7.0
6.5
6.0
5.5
5.0
4.5
4.0
3.5
ppm
2.00
2.00

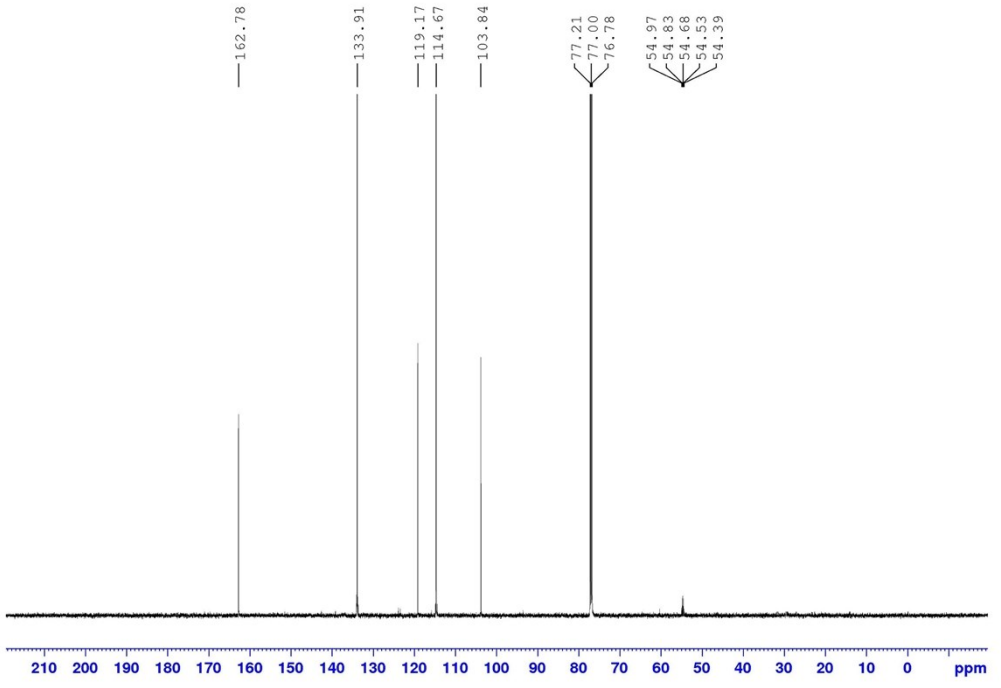
162.78
133.91
119.17
114.67
103.84
77.21
77.00
76.78
54.97
54.83
54.68
54.53
54.39
210
200
190
180
170
160
150
140
130
120
110
100
90
80
70
60
50
40
30
20
10
0
ppm

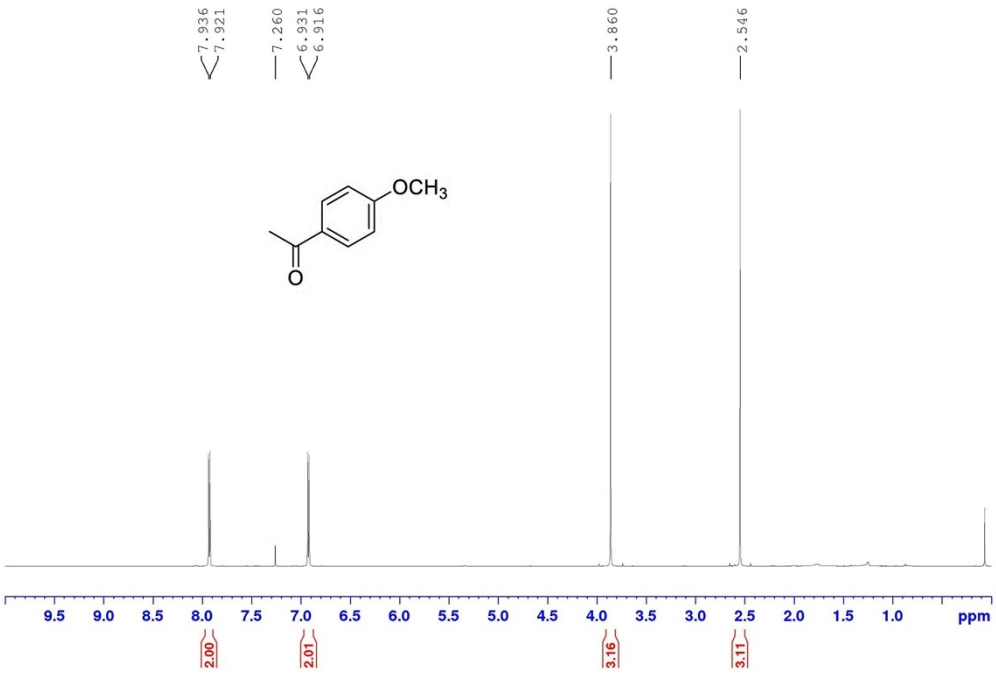
7.936
7.921
7.260
6.931
6.916
3.860
2.546
OCH3
O
9.5 9.0 8.5 8.0 7.5 7.0 6.5 6.0 5.5 5.0 4.5 4.0 3.5 3.0 2.5 2.0 1.5 1.0 ppm
2.00
2.01
3.16
3.11

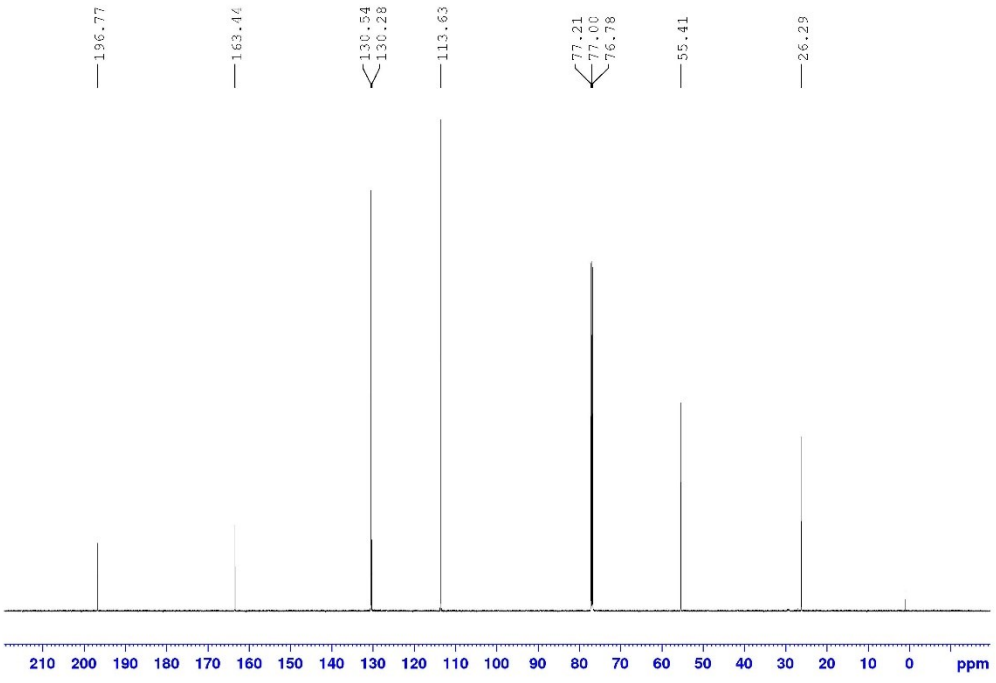
196.77
163.44
130.54
130.28
113.63
77.21
77.00
76.78
55.41
26.29
210 200 190 180 170 160 150 140 130 120 110 100 90 80 70 60 50 40 30 20 10 0 ppm

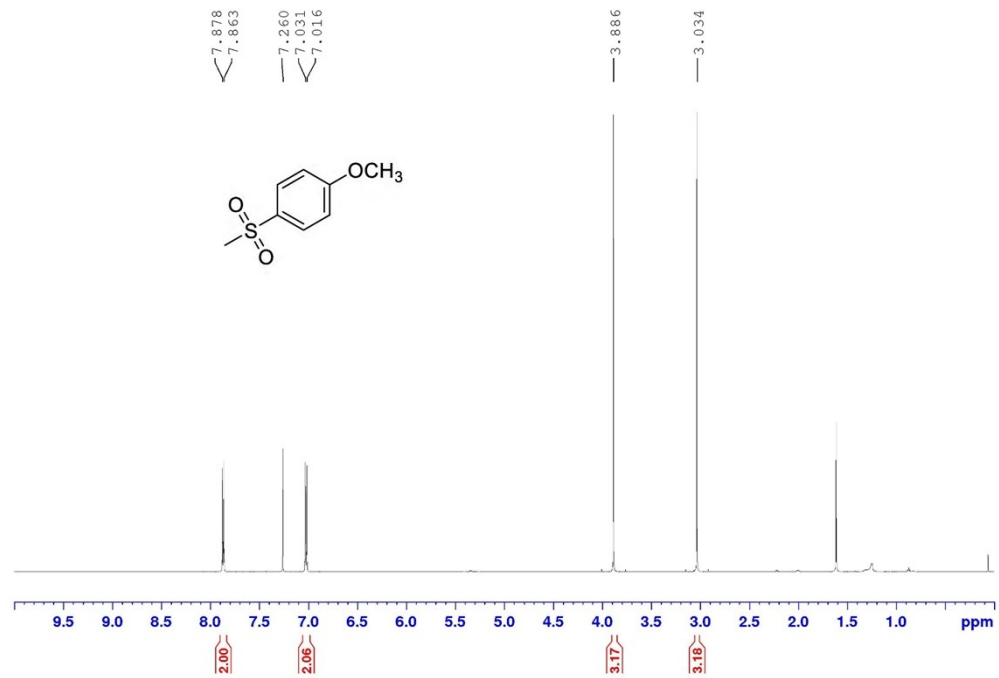
7.878
7.863
7.260
7.031
7.016
3.886
3.034
OCH3
O
S
O
9.5 9.0 8.5 8.0 7.5 7.0 6.5 6.0 5.5 5.0 4.5 4.0 3.5 3.0 2.5 2.0 1.5 1.0 ppm
2.00
2.06
3.17
3.18

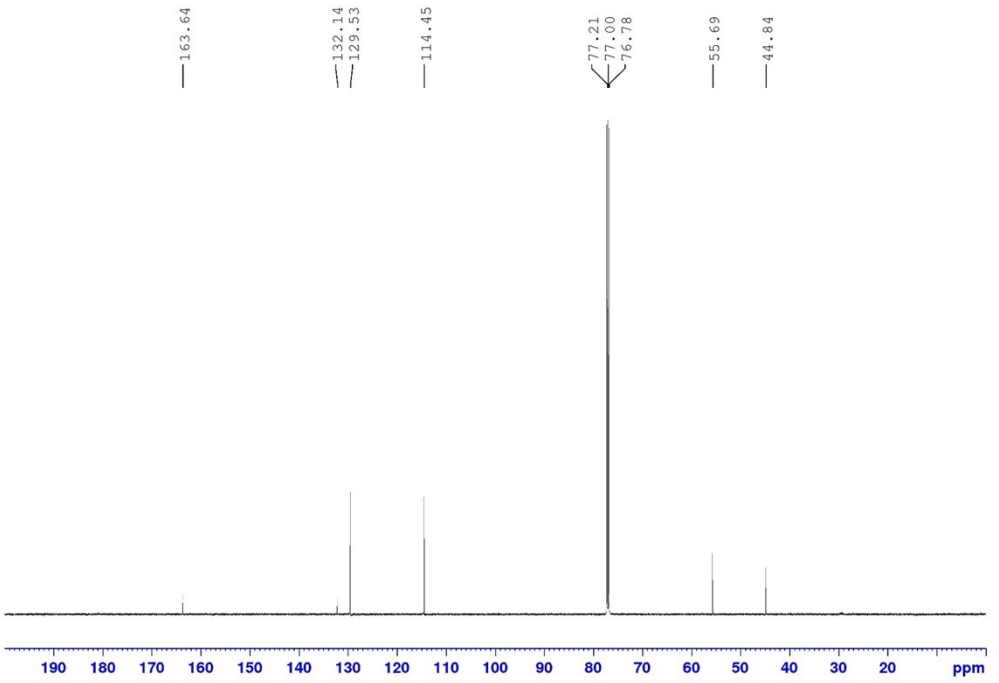
163.64
132.14
129.53
114.45
77.21
77.00
76.78
55.69
44.84
190 180 170 160 150 140 130 120 110 100 90 80 70 60 50 40 30 20 ppm

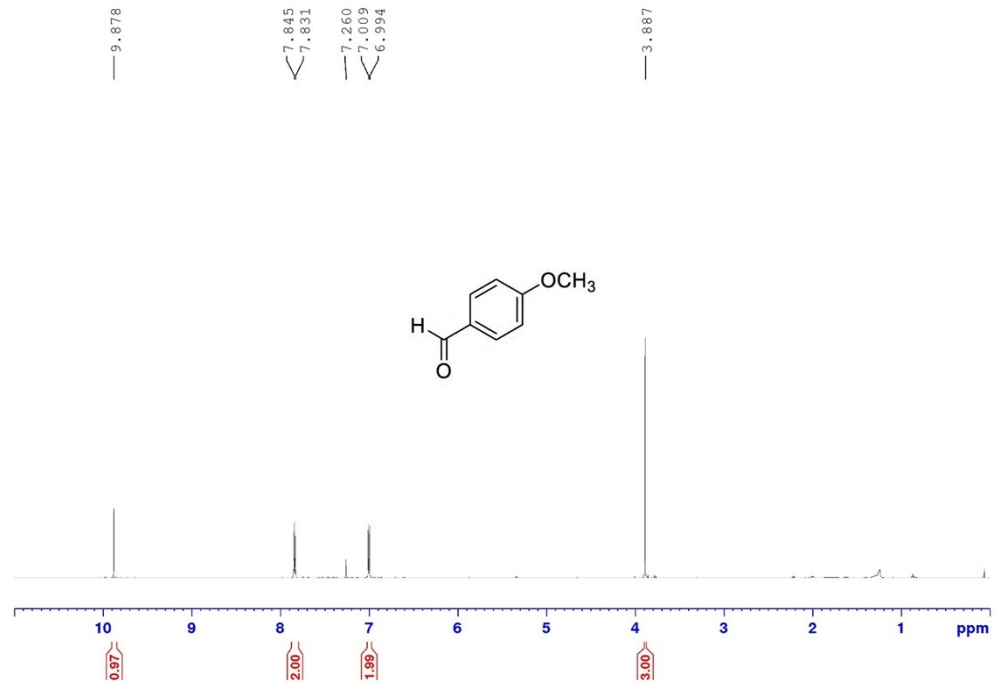
9.878
7.845
7.831
7.260
7.009
6.994
3.887
OCH3
H
O
10
9
8
7
6
5
4
3
2
1
ppm
0.97
2.00
1.99
3.00

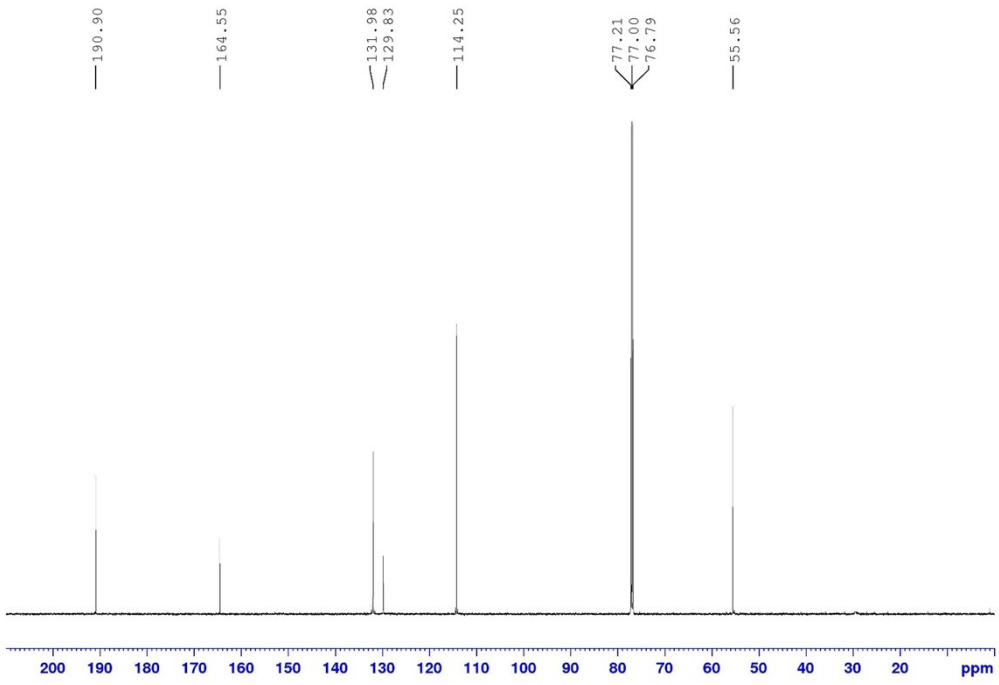
190.90
164.55
131.98
129.83
114.25
77.21
77.00
76.79
55.56
200
190
180
170
160
150
140
130
120
110
100
90
80
70
60
50
40
30
20
ppm

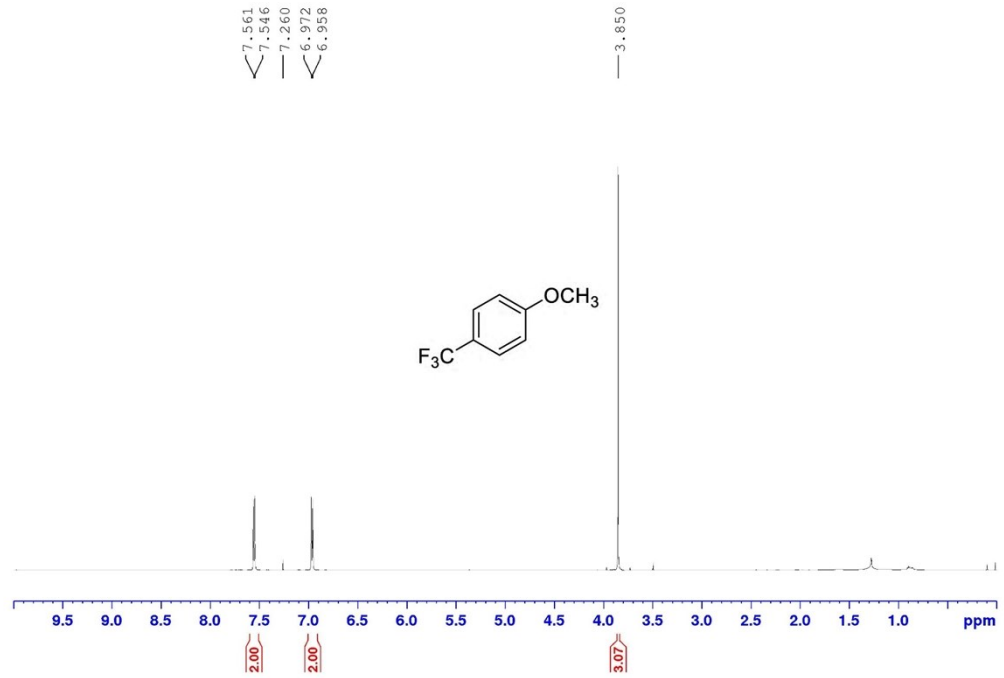
7.561
7.546
7.260
6.972
6.958
3.850
OCH3
F3C
9.5 9.0 8.5 8.0 7.5 7.0 6.5 6.0 5.5 5.0 4.5 4.0 3.5 3.0 2.5 2.0 1.5 1.0 ppm
2.00
2.00
3.07

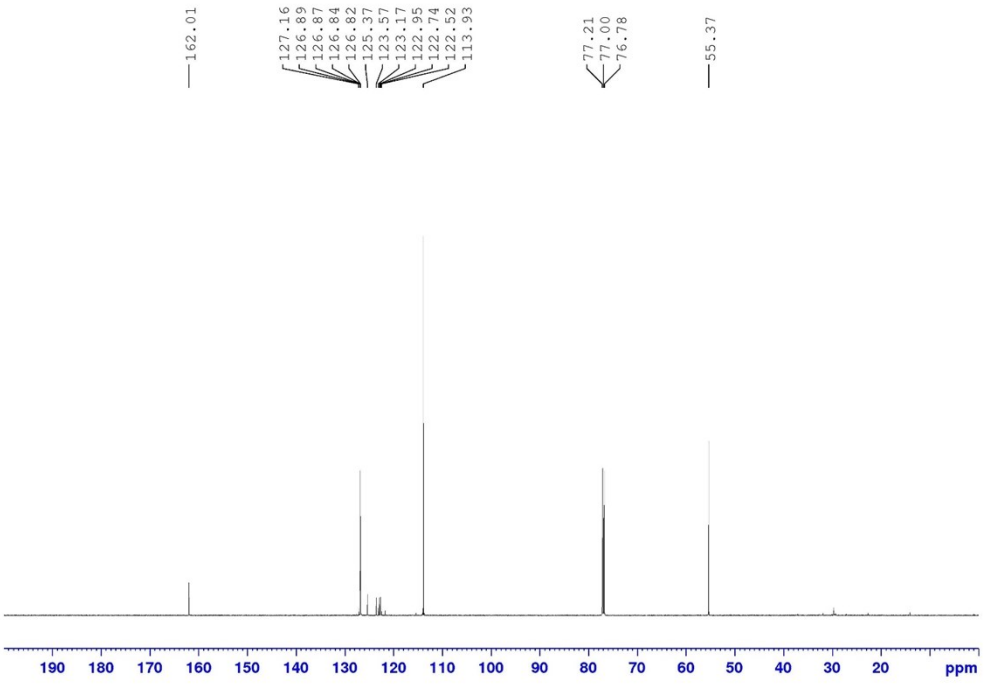
162.01
127.16
126.89
126.87
126.84
126.82
125.37
123.57
123.17
122.95
122.74
122.52
113.93
77.21
77.00
76.78
55.37
190 180 170 160 150 140 130 120 110 100 90 80 70 60 50 40 30 20 ppm

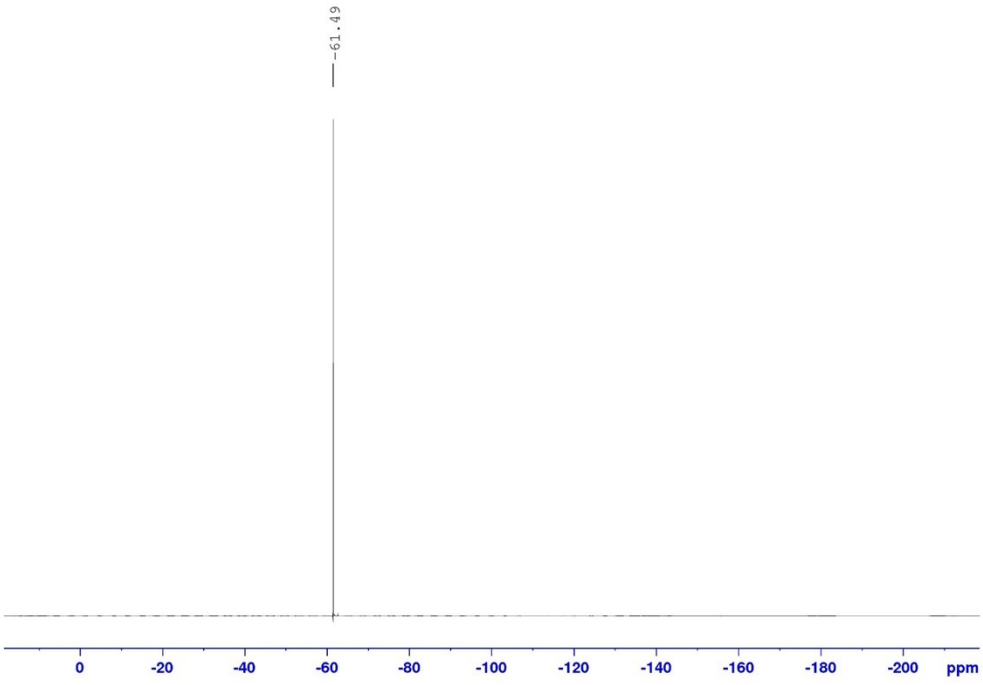
-61.49
0
-20
-40
-60
-80
-100
-120
-140
-160
-180
-200
ppm

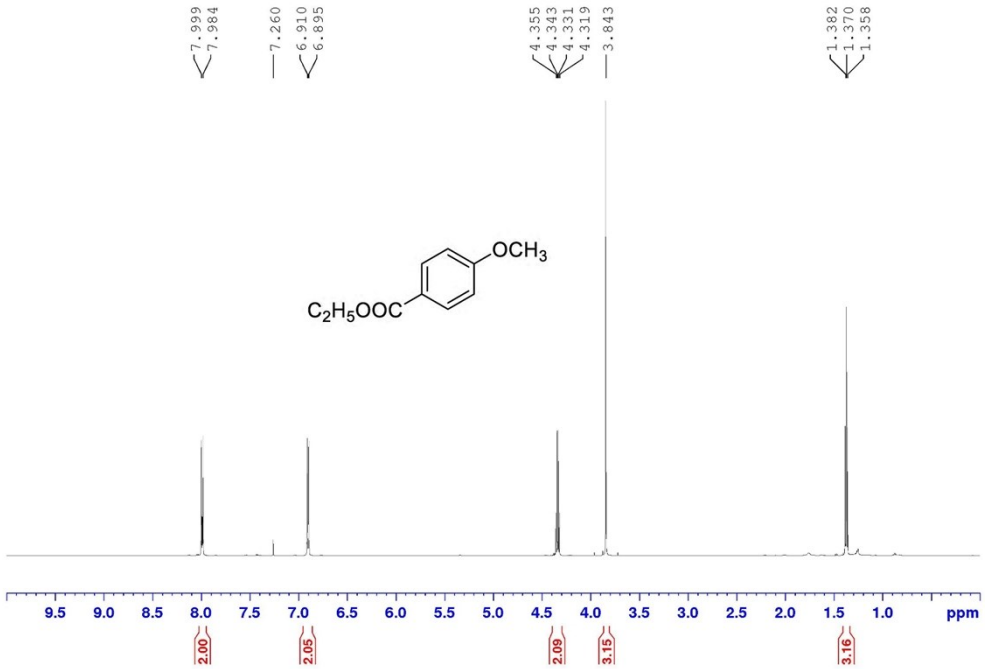
7.999
7.984
7.260
6.910
6.895
4.355
4.343
4.331
4.319
3.843
1.382
1.370
1.358
OCH3
C2H5OOC
9.5 9.0 8.5 8.0 7.5 7.0 6.5 6.0 5.5 5.0 4.5 4.0 3.5 3.0 2.5 2.0 1.5 1.0 ppm
2.00
2.05
2.09
3.15
3.16

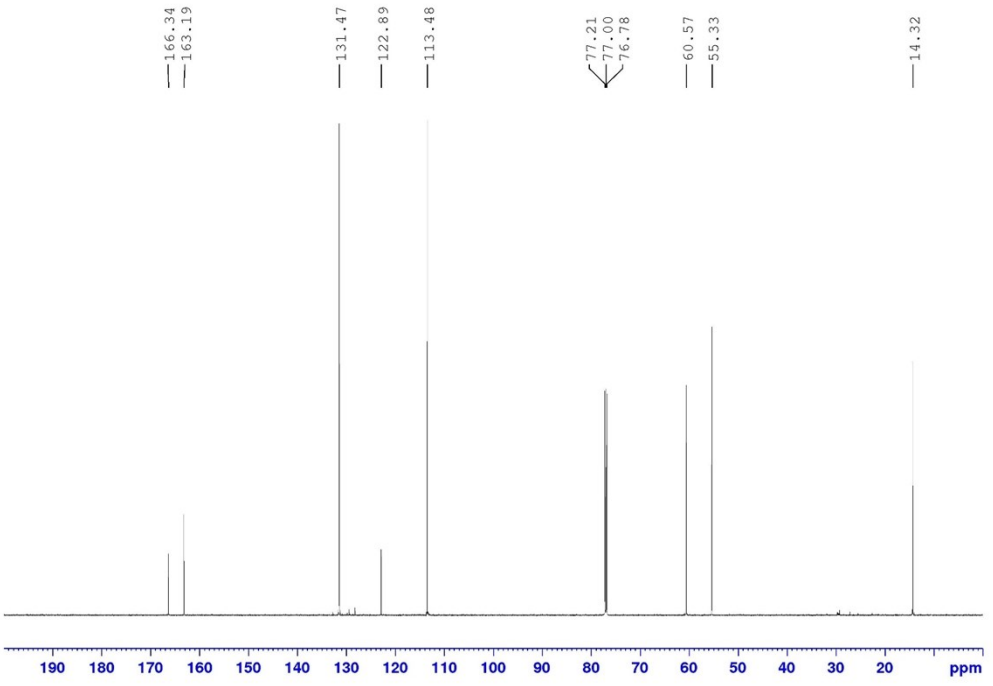
166.34
163.19
131.47
122.89
113.48
77.21
77.00
76.78
60.57
55.33
14.32
190 180 170 160 150 140 130 120 110 100 90 80 70 60 50 40 30 20 ppm

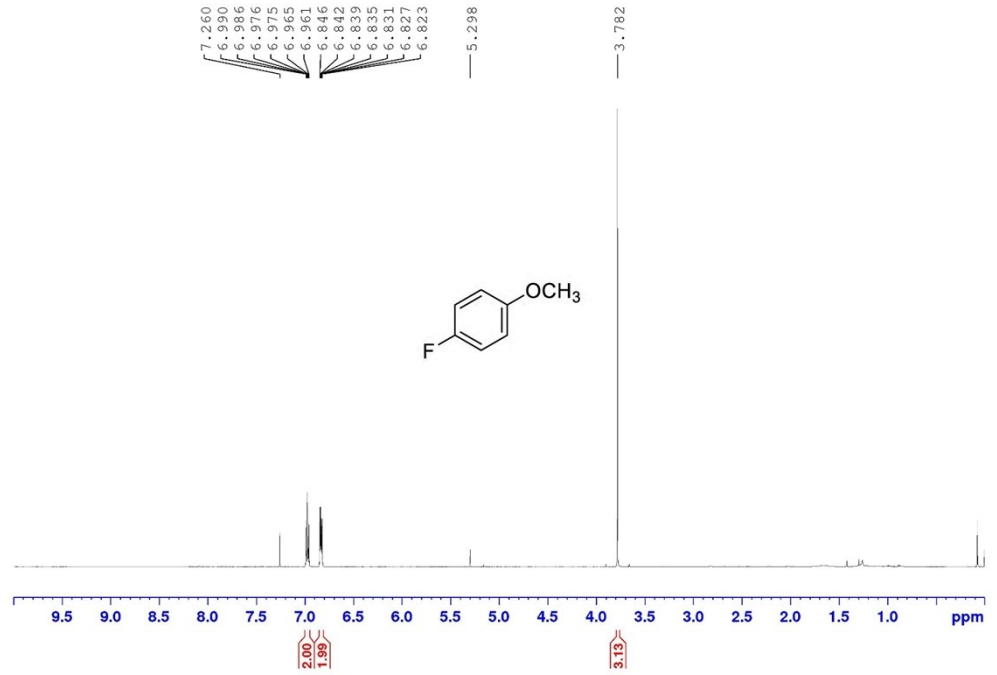
7.260
6.990
6.986
6.976
6.975
6.965
6.961
6.846
6.842
6.839
6.835
6.831
6.827
6.823
5.298
3.782
OCH3
F
9.5 9.0 8.5 8.0 7.5 7.0 6.5 6.0 5.5 5.0 4.5 4.0 3.5 3.0 2.5 2.0 1.5 1.0 ppm
2.00
1.99
3.13

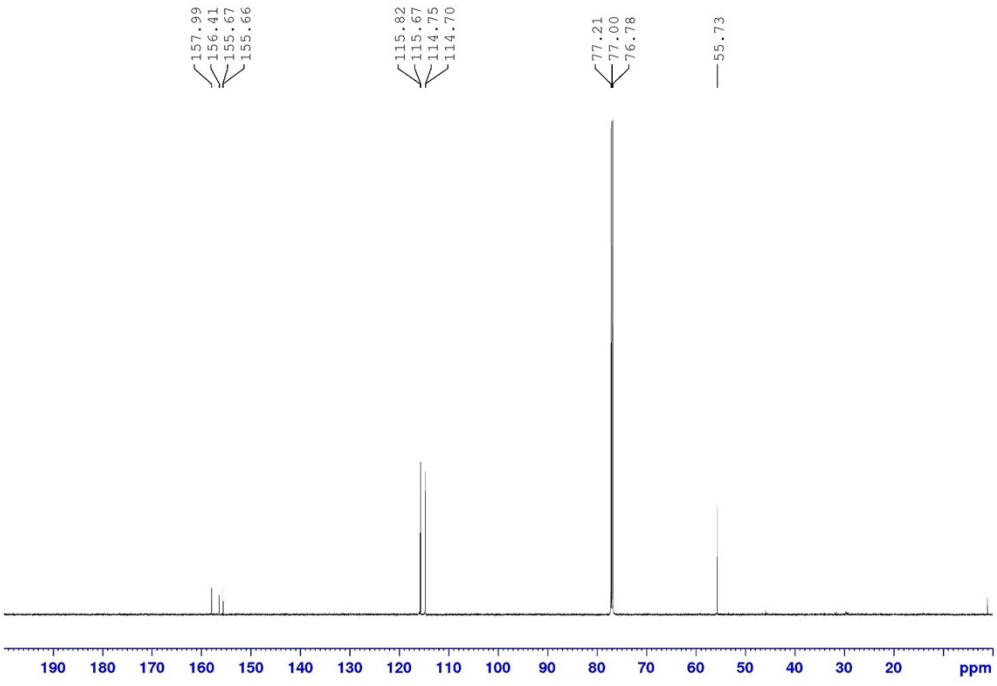
157.99
156.41
155.67
155.66
115.82
115.67
114.75
114.70
77.21
77.00
76.78
55.73
190 180 170 160 150 140 130 120 110 100 90 80 70 60 50 40 30 20 ppm

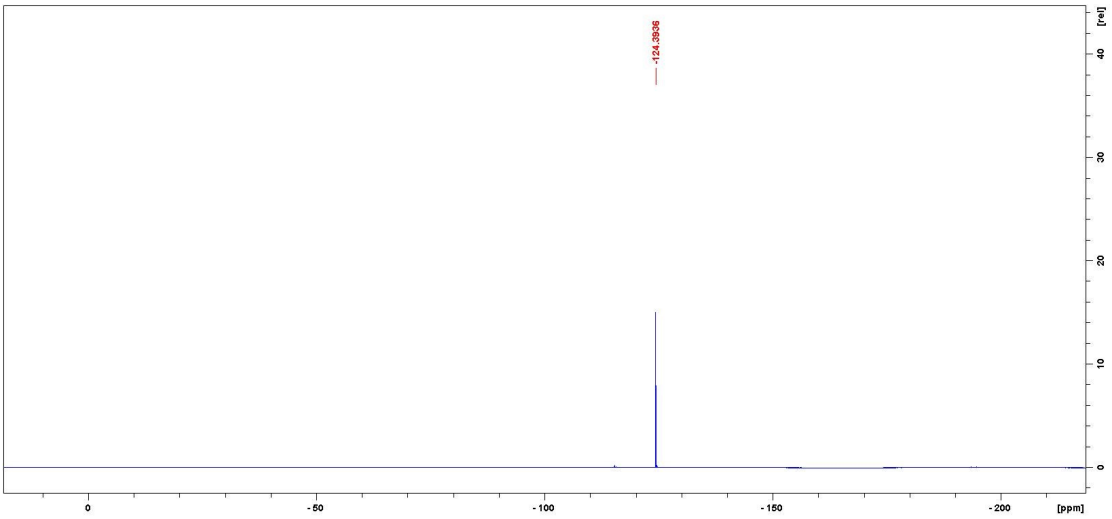
-124.3936
[rel]
40
30
20
10
0
0
-50
-100
-150
-200
[ppm]

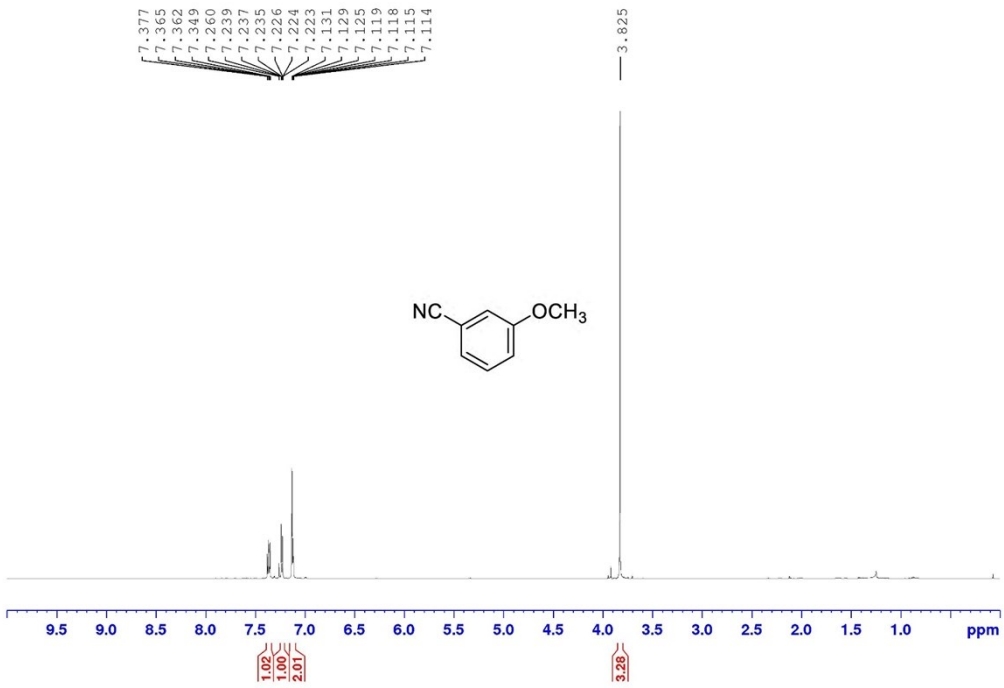
7.377
7.365
7.362
7.349
7.260
7.239
7.237
7.235
7.226
7.224
7.223
7.131
7.129
7.125
7.119
7.118
7.115
7.114
3.825
NC
OCH3
9.5 9.0 8.5 8.0 7.5 7.0 6.5 6.0 5.5 5.0 4.5 4.0 3.5 3.0 2.5 2.0 1.5 1.0 ppm
1.02
1.00
2.01
3.28

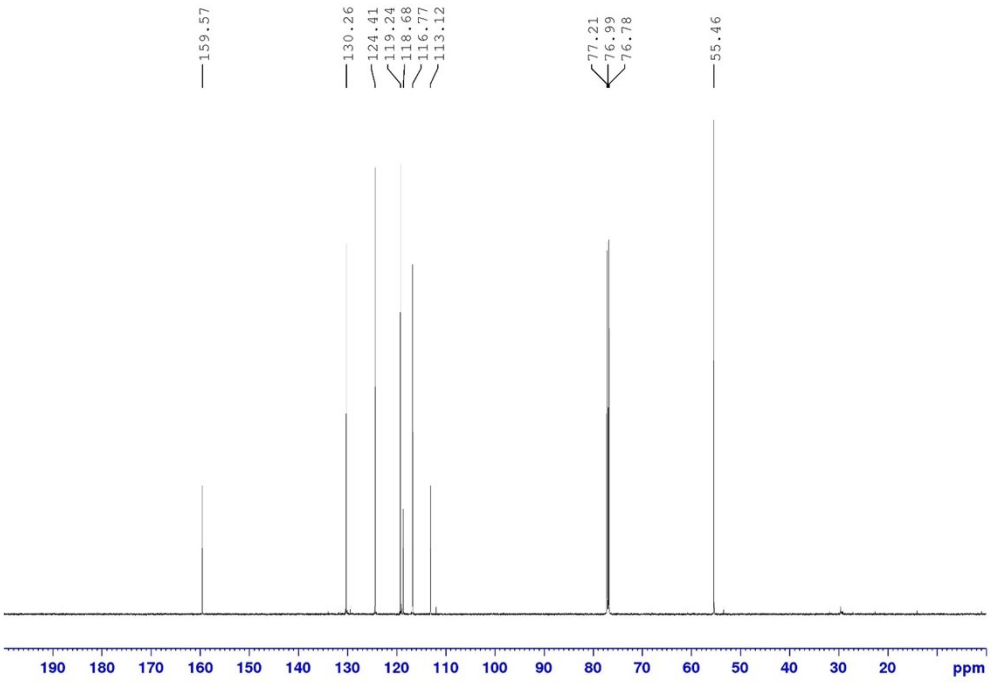
159.57
130.26
124.41
119.24
118.68
116.77
113.12
77.21
76.99
76.78
55.46
190 180 170 160 150 140 130 120 110 100 90 80 70 60 50 40 30 20 ppm

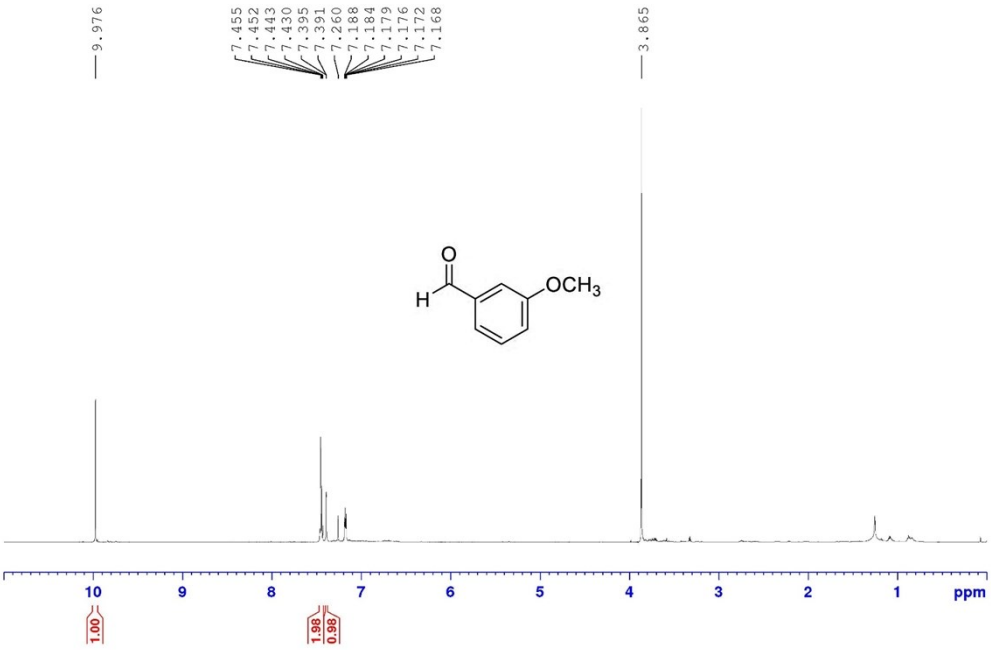
9.976
7.455
7.452
7.443
7.430
7.395
7.391
7.260
7.188
7.184
7.179
7.176
7.172
7.168
3.865
O
H
OCH3
10
9
8
7
6
5
4
3
2
1
ppm
1.00
1.98
0.98

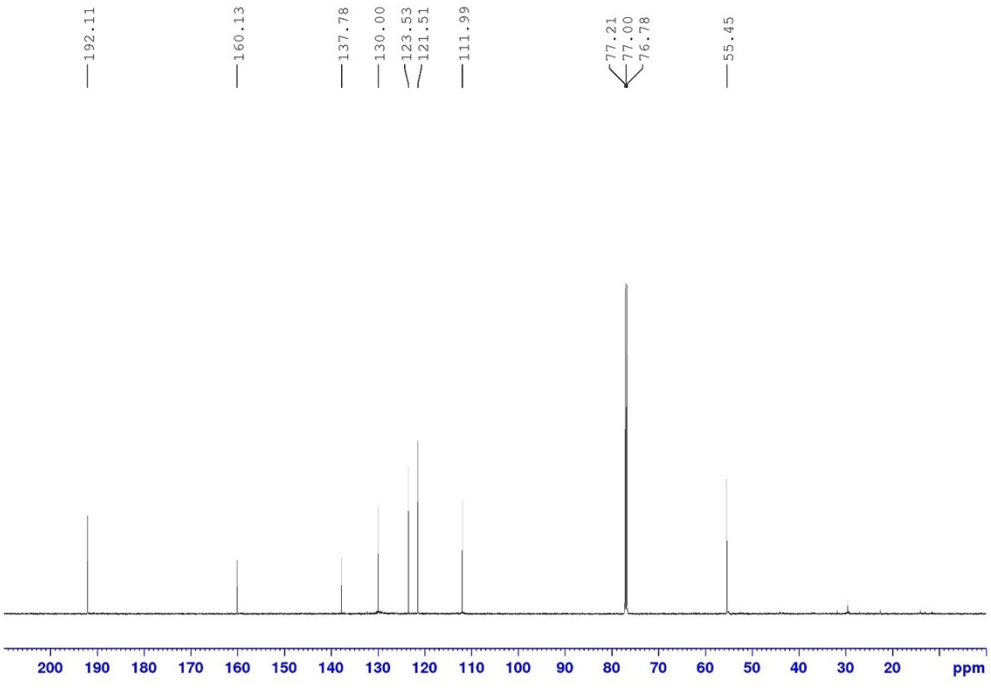
192.11
160.13
137.78
130.00
123.53
121.51
111.99
77.21
77.00
76.78
55.45
200
190
180
170
160
150
140
130
120
110
100
90
80
70
60
50
40
30
20
ppm

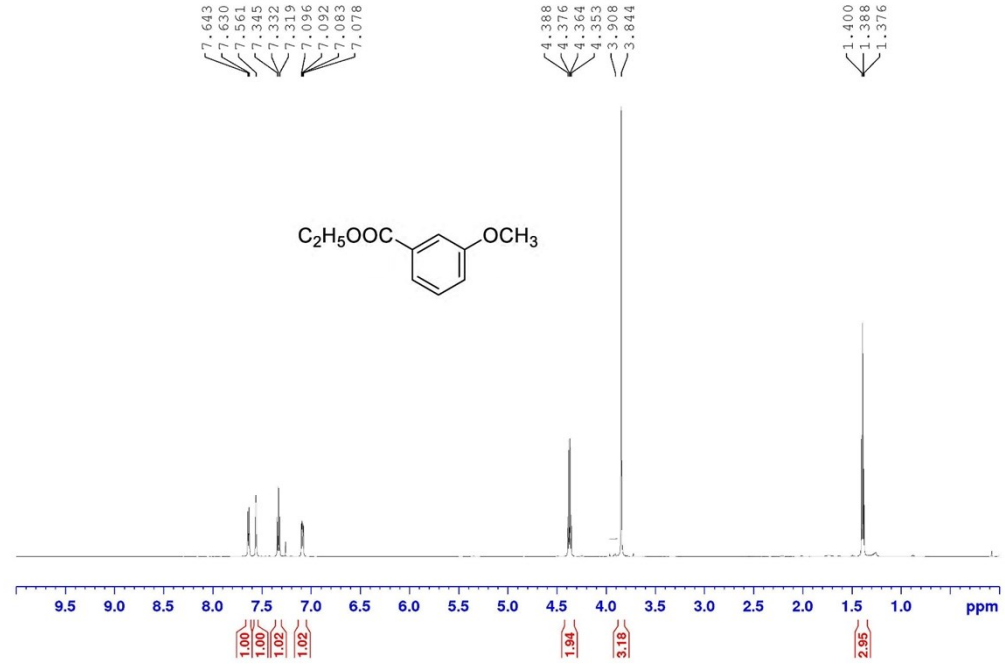
7.643
7.630
7.561
7.345
7.332
7.319
7.096
7.092
7.083
7.078
4.388
4.376
4.364
4.353
3.908
3.844
1.400
1.388
1.376
C2H5OOC
OCH3
9.5 9.0 8.5 8.0 7.5 7.0 6.5 6.0 5.5 5.0 4.5 4.0 3.5 3.0 2.5 2.0 1.5 1.0 ppm
1.00
1.00
1.02
1.02
1.94
3.18
2.95

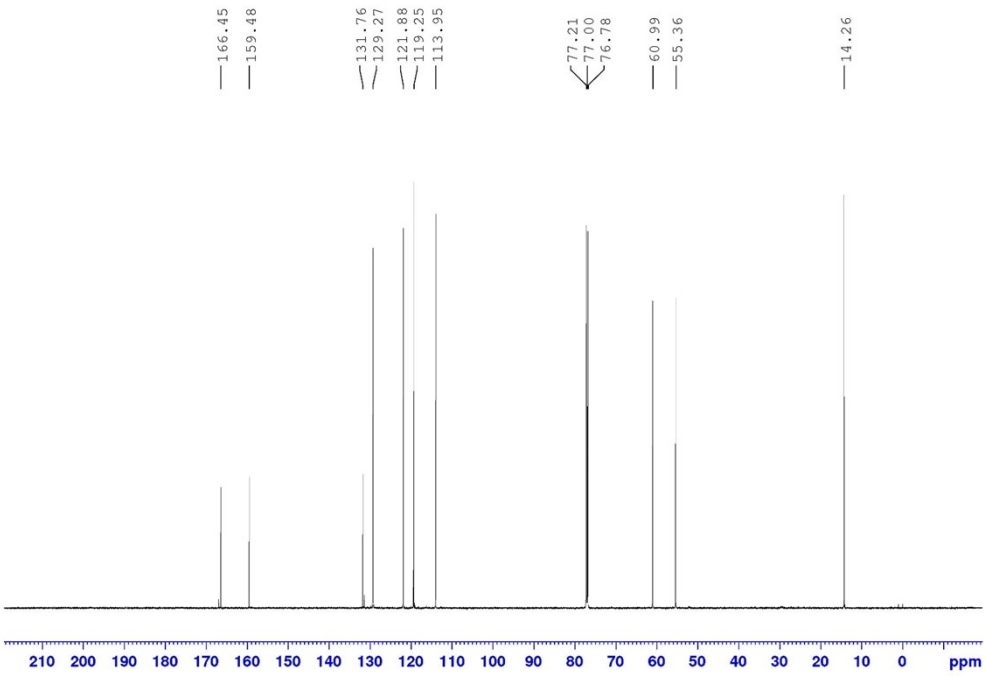
166.45
159.48
131.76
129.27
121.88
119.25
113.95
77.21
77.00
76.78
60.99
55.36
14.26
210 200 190 180 170 160 150 140 130 120 110 100 90 80 70 60 50 40 30 20 10 0 ppm

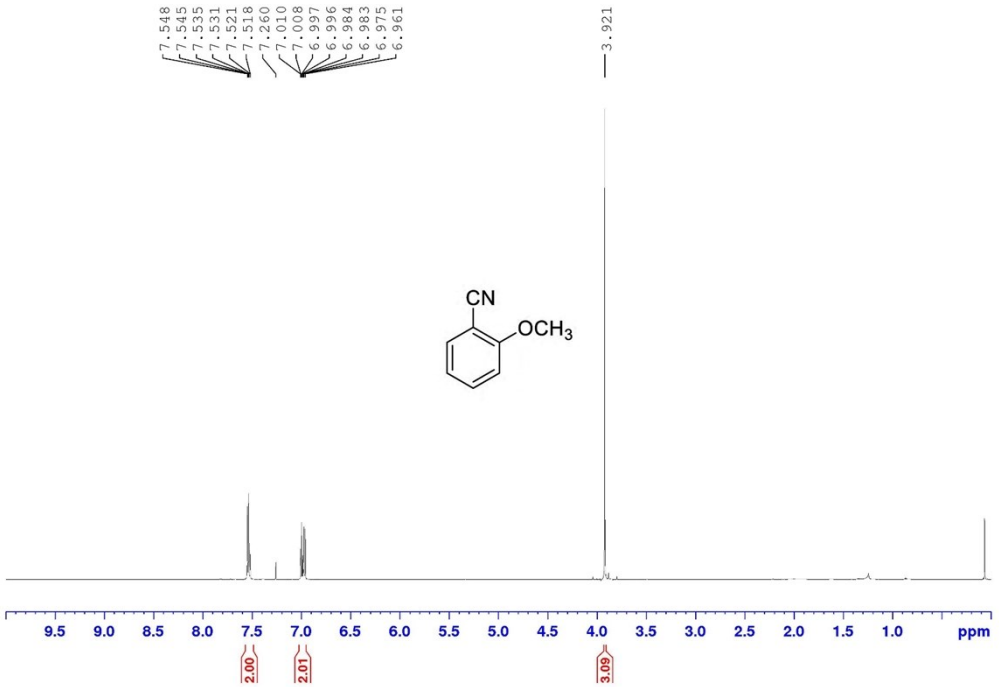
7.548
7.545
7.535
7.531
7.521
7.518
7.260
7.010
7.008
6.997
6.996
6.984
6.983
6.975
6.961
3.921
CN
OCH3
9.5 9.0 8.5 8.0 7.5 7.0 6.5 6.0 5.5 5.0 4.5 4.0 3.5 3.0 2.5 2.0 1.5 1.0 ppm
2.00
2.01
3.09

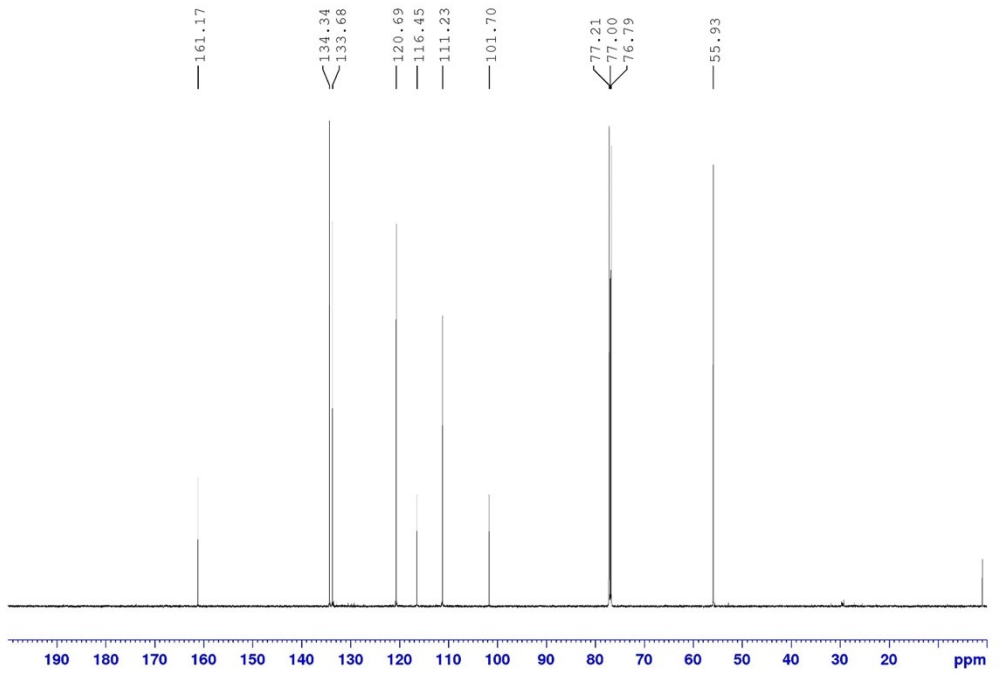
161.17
134.34
133.68
120.69
116.45
111.23
101.70
77.21
77.00
76.79
55.93
190 180 170 160 150 140 130 120 110 100 90 80 70 60 50 40 30 20 ppm

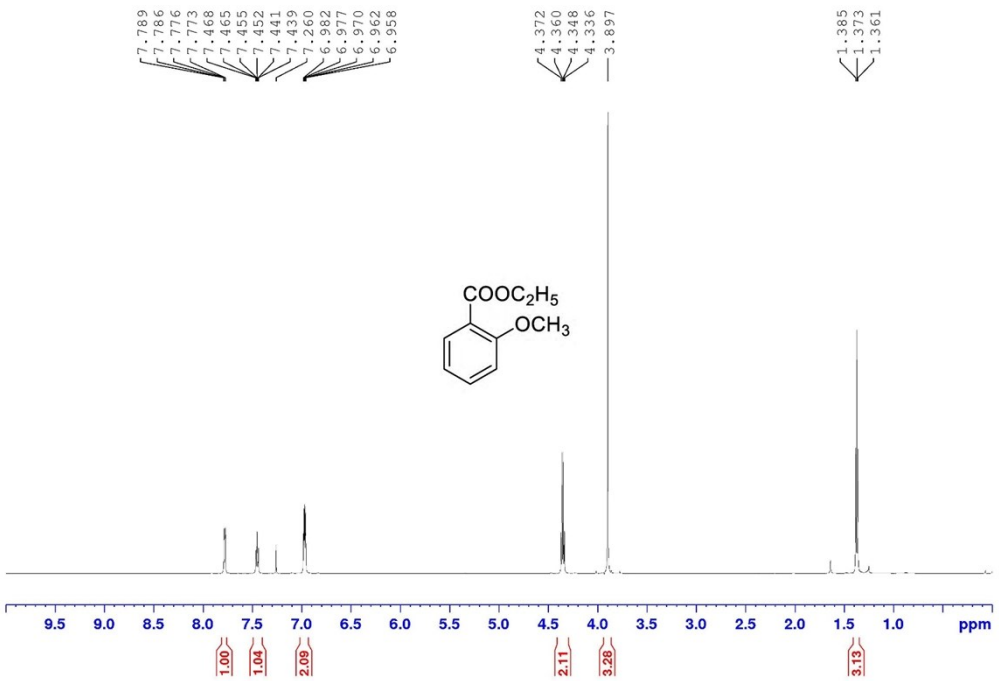
7.789
7.786
7.776
7.773
7.468
7.465
7.455
7.452
7.441
7.439
7.260
6.982
6.977
6.970
6.962
6.958
4.372
4.360
4.348
4.336
3.897
1.385
1.373
1.361
COOC2H5
OCH3
9.5 9.0 8.5 8.0 7.5 7.0 6.5 6.0 5.5 5.0 4.5 4.0 3.5 3.0 2.5 2.0 1.5 1.0 ppm
1.00
1.04
2.09
2.11
3.28
3.13

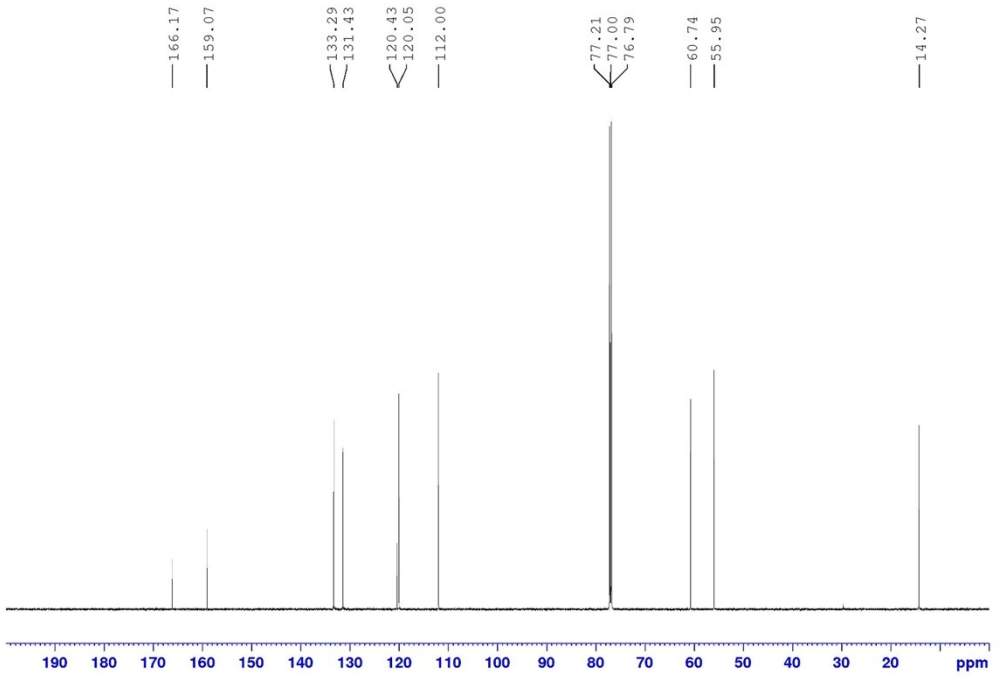
166.17
159.07
133.29
131.43
120.43
120.05
112.00
77.21
77.00
76.79
60.74
55.95
14.27
190 180 170 160 150 140 130 120 110 100 90 80 70 60 50 40 30 20 ppm

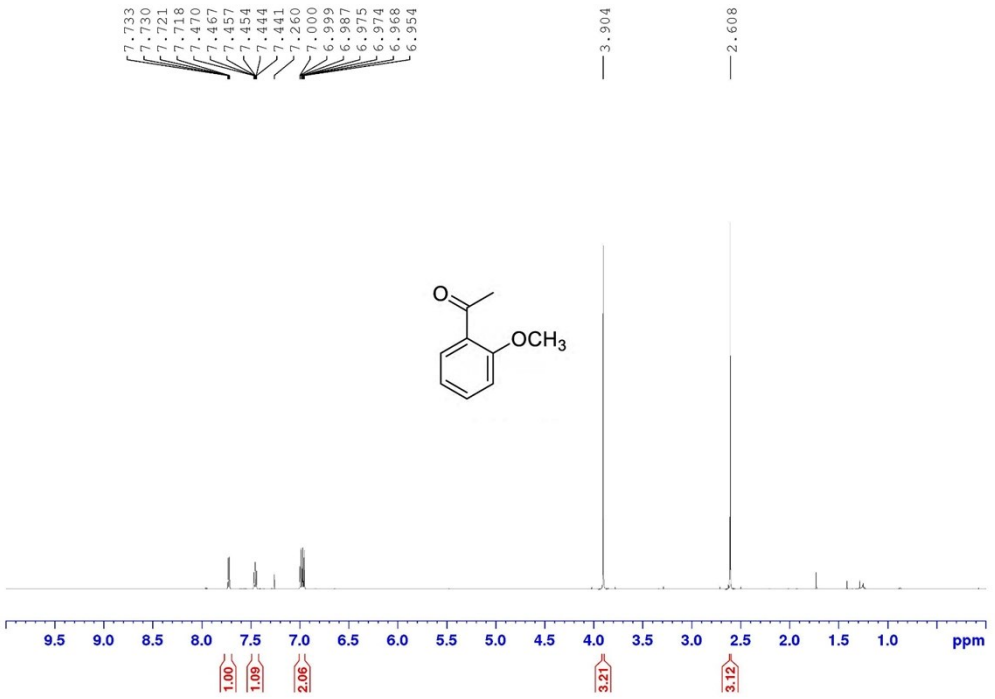
7.733
7.730
7.721
7.718
7.470
7.467
7.457
7.454
7.444
7.441
7.260
7.000
6.999
6.987
6.975
6.974
6.968
6.954
3.904
2.608
O
OCH3
9.5 9.0 8.5 8.0 7.5 7.0 6.5 6.0 5.5 5.0 4.5 4.0 3.5 3.0 2.5 2.0 1.5 1.0 ppm
1.00
1.09
2.06
3.21
3.12

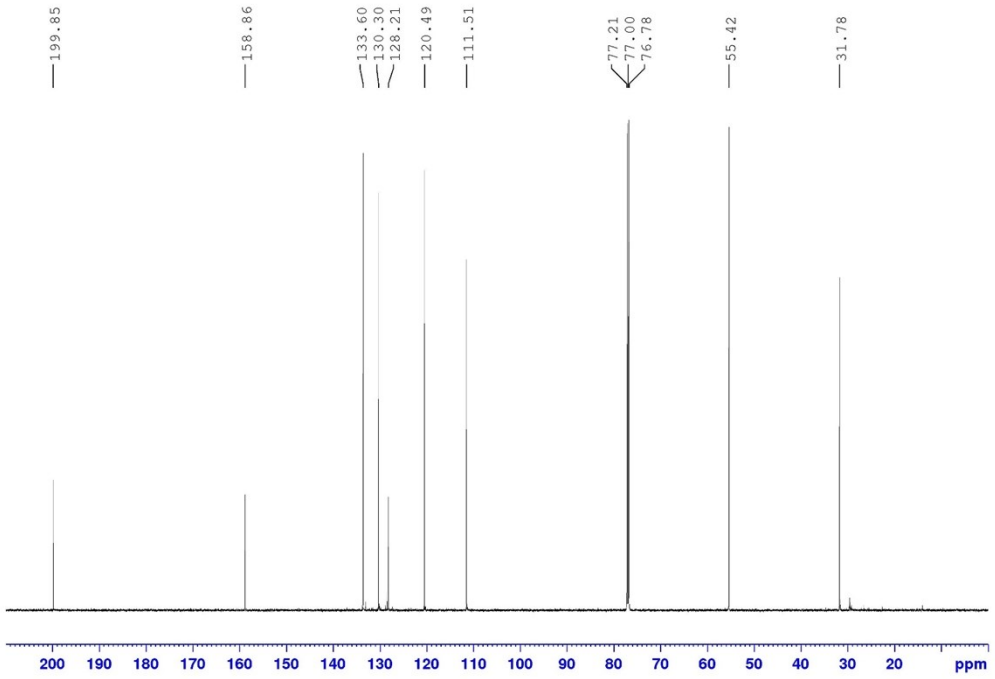
199.85
158.86
133.60
130.30
128.21
120.49
111.51
77.21
77.00
76.78
55.42
31.78
200 190 180 170 160 150 140 130 120 110 100 90 80 70 60 50 40 30 20 ppm

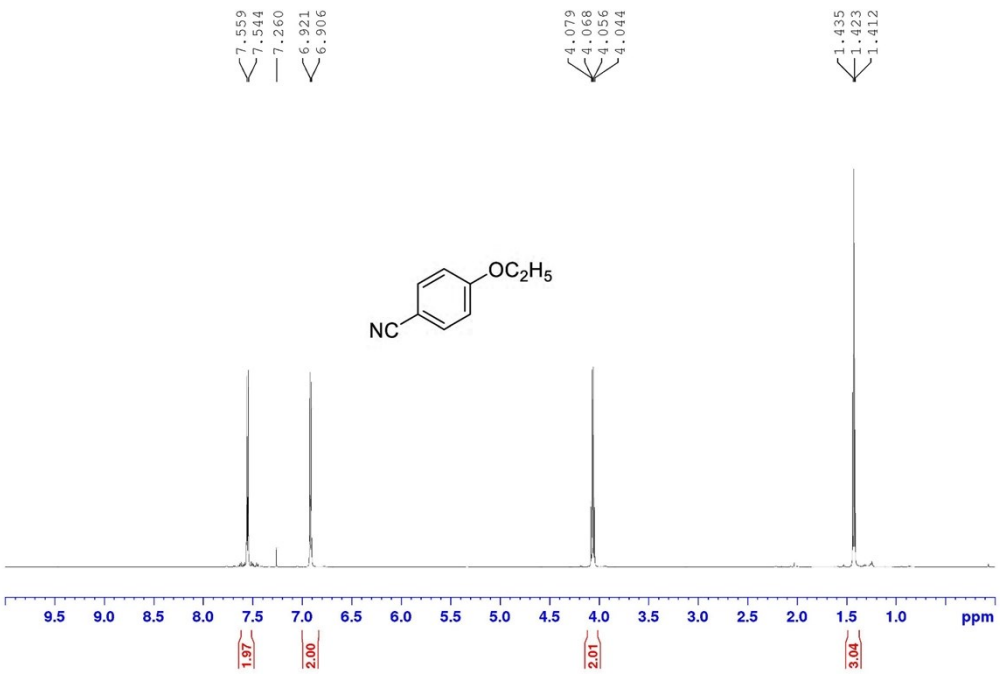
7.559
7.544
7.260
6.921
6.906
4.079
4.068
4.056
4.044
1.435
1.423
1.412
OC2H5
NC
9.5 9.0 8.5 8.0 7.5 7.0 6.5 6.0 5.5 5.0 4.5 4.0 3.5 3.0 2.5 2.0 1.5 1.0 ppm
1.97
2.00
2.01
3.04

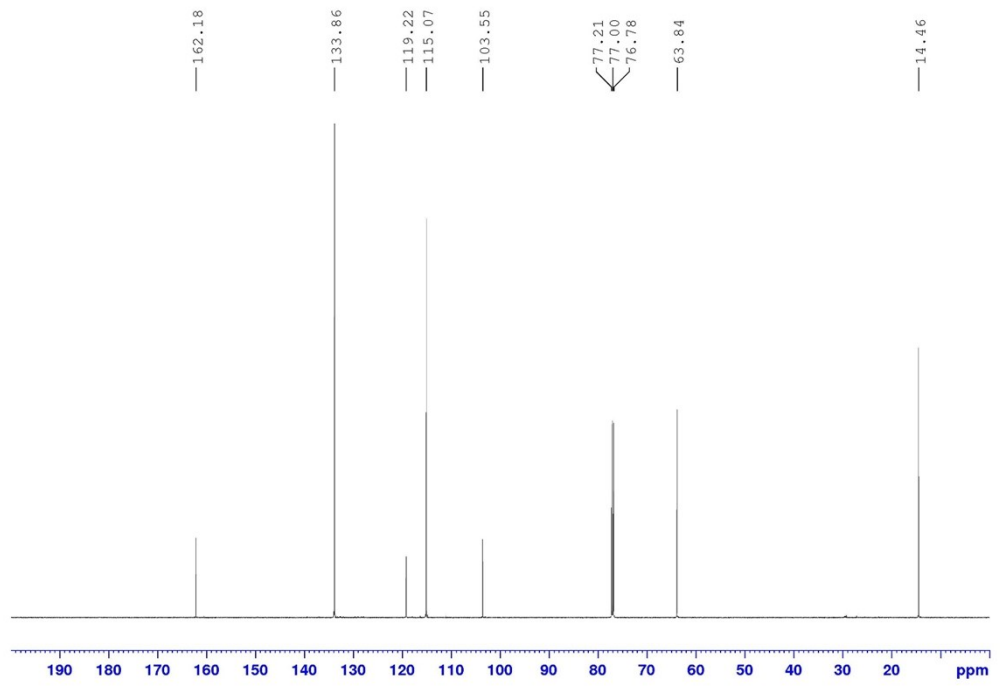
162.18
133.86
119.22
115.07
103.55
77.21
77.00
76.78
63.84
14.46
190 180 170 160 150 140 130 120 110 100 90 80 70 60 50 40 30 20 ppm

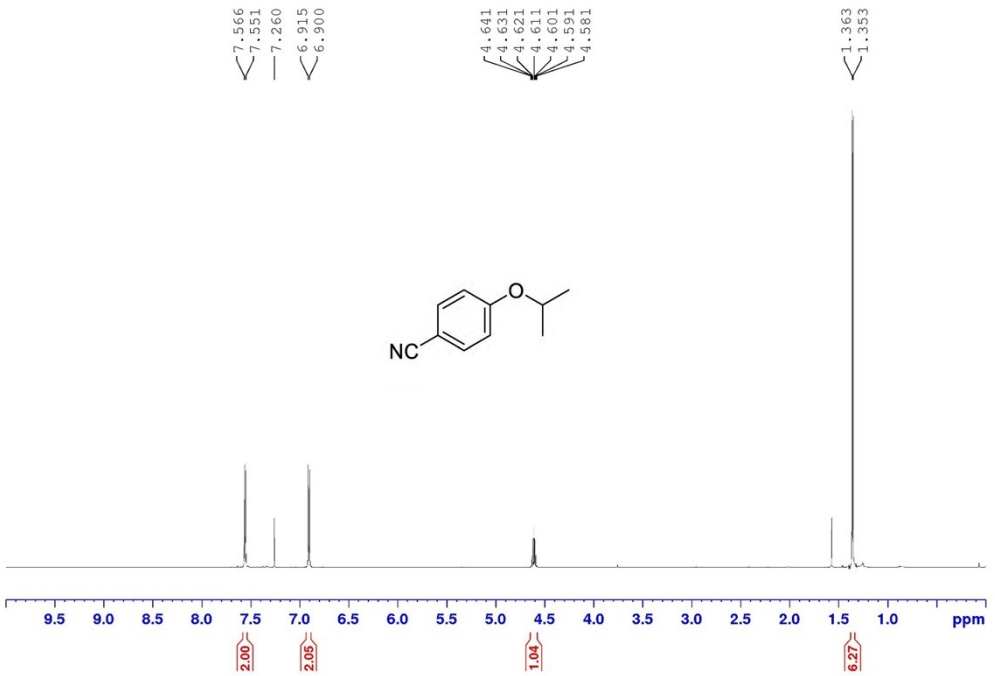
7.566
7.551
7.260
6.915
6.900
4.641
4.631
4.621
4.611
4.601
4.591
4.581
1.363
1.353
O
NC
9.5 9.0 8.5 8.0 7.5 7.0 6.5 6.0 5.5 5.0 4.5 4.0 3.5 3.0 2.5 2.0 1.5 1.0 ppm
2.00
2.05
1.04
6.27

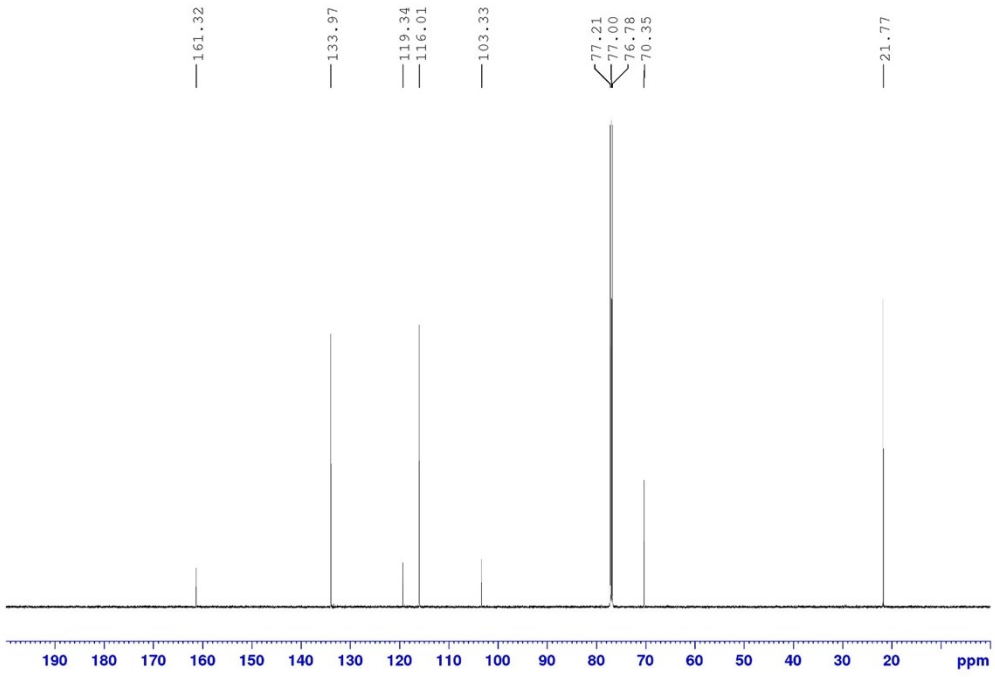
161.32
133.97
119.34
116.01
103.33
77.21
77.00
76.78
70.35
21.77
190 180 170 160 150 140 130 120 110 100 90 80 70 60 50 40 30 20 ppm

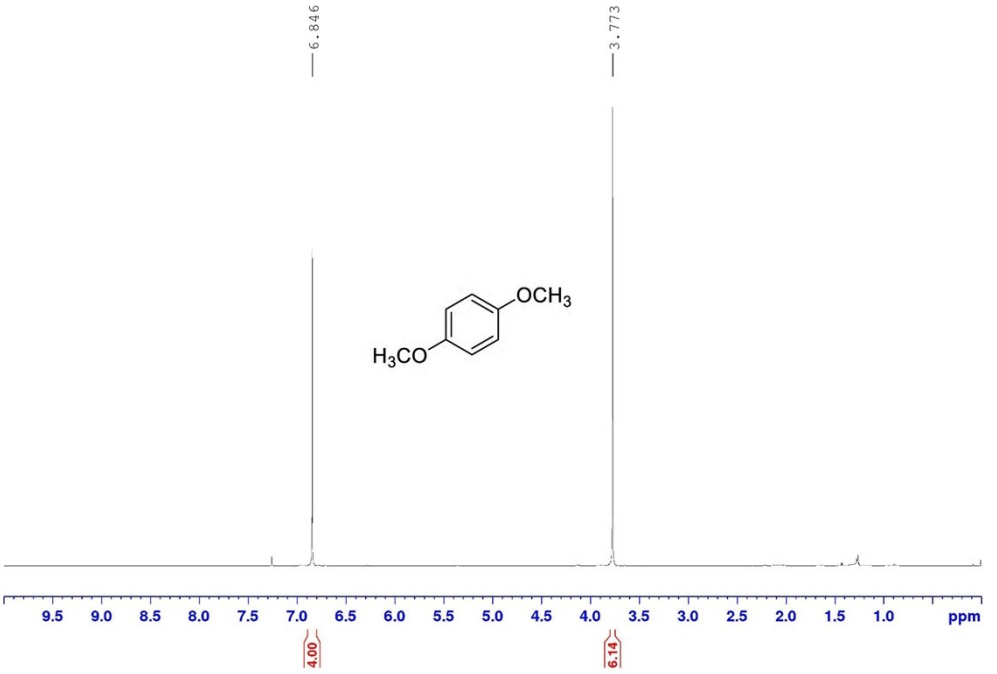
6.846
3.773
OCH3
H3CO
9.5 9.0 8.5 8.0 7.5 7.0 6.5 6.0 5.5 5.0 4.5 4.0 3.5 3.0 2.5 2.0 1.5 1.0 ppm
4.00
6.14

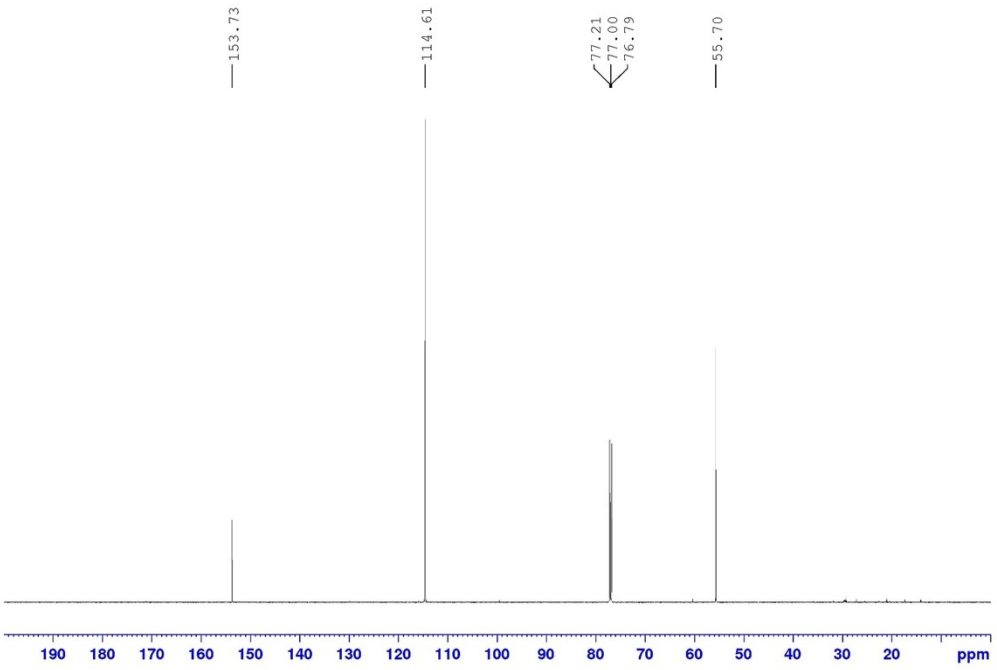
153.73
114.61
77.21
77.00
76.79
55.70
190 180 170 160 150 140 130 120 110 100 90 80 70 60 50 40 30 20 ppm

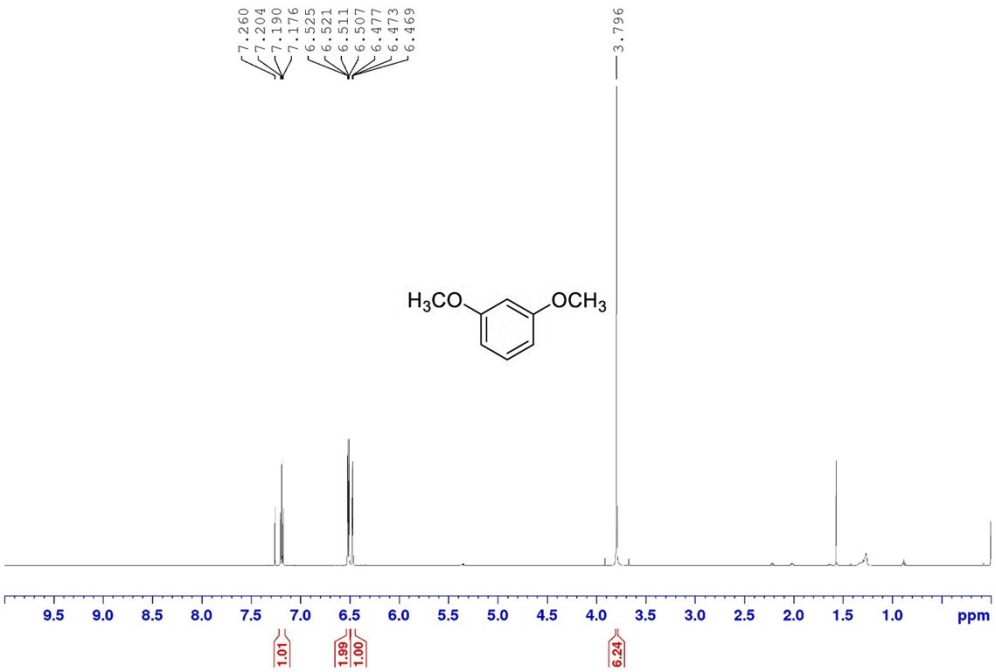
7.260
7.204
7.190
7.176
6.525
6.521
6.511
6.507
6.477
6.473
6.469
3.796
H3CO
OCH3
9.5 9.0 8.5 8.0 7.5 7.0 6.5 6.0 5.5 5.0 4.5 4.0 3.5 3.0 2.5 2.0 1.5 1.0 ppm
1.01
1.99
1.00
6.24

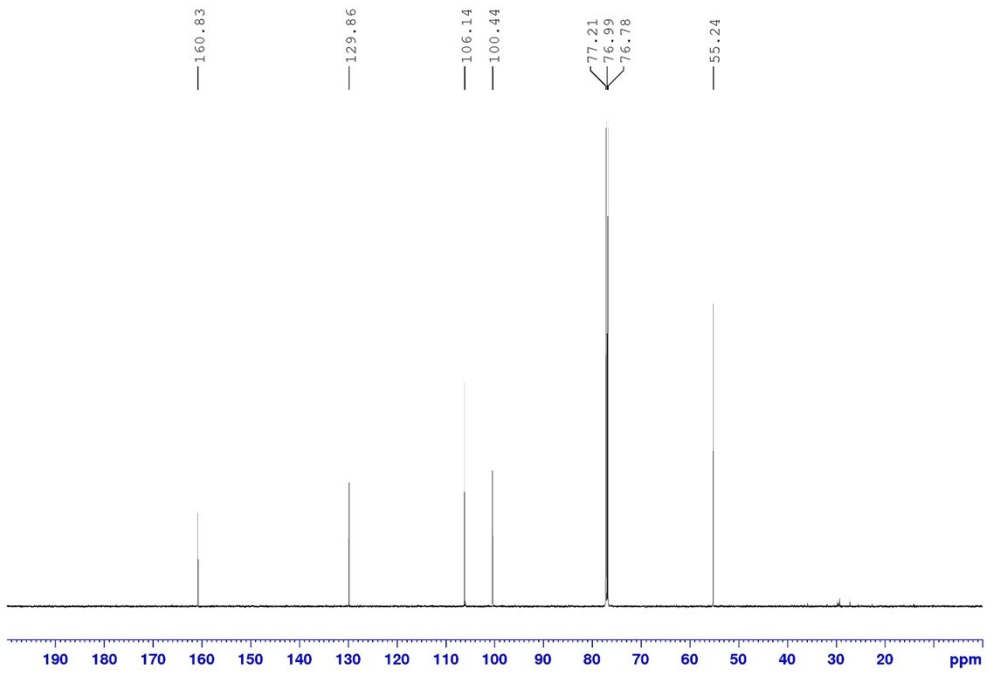
160.83
129.86
106.14
100.44
77.21
76.99
76.78
55.24
190 180 170 160 150 140 130 120 110 100 90 80 70 60 50 40 30 20 ppm

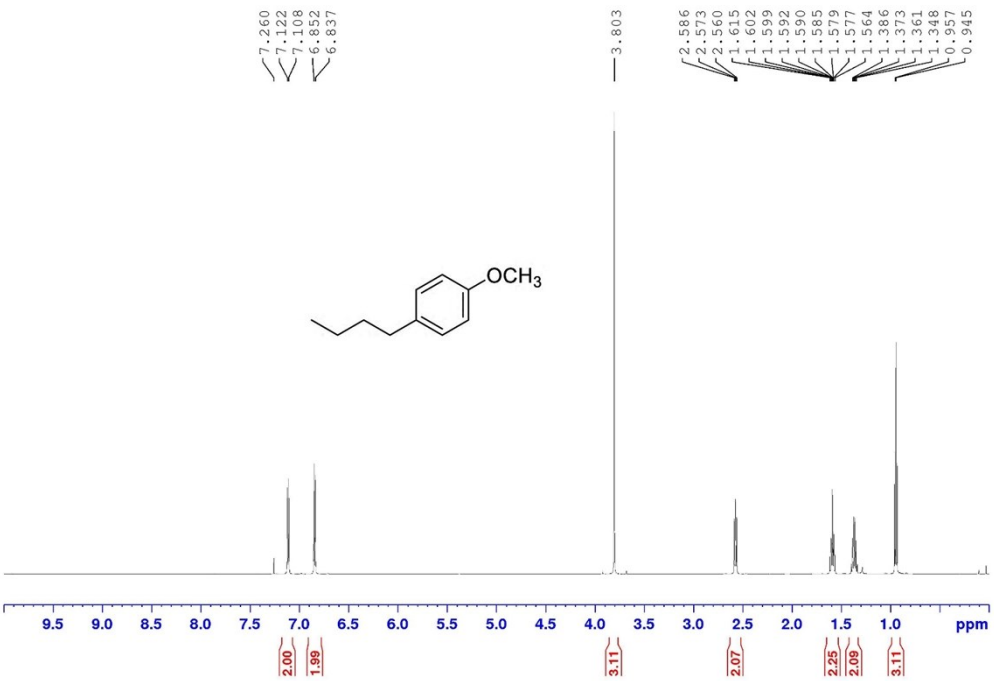
7.260
7.122
7.108
6.852
6.837
3.803
2.586
2.573
2.560
1.615
1.602
1.599
1.592
1.590
1.585
1.579
1.577
1.564
1.386
1.373
1.361
1.348
0.957
0.945
OCH3
9.5 9.0 8.5 8.0 7.5 7.0 6.5 6.0 5.5 5.0 4.5 4.0 3.5 3.0 2.5 2.0 1.5 1.0 ppm
2.00
1.99
3.11
2.07
2.25
2.09
3.11

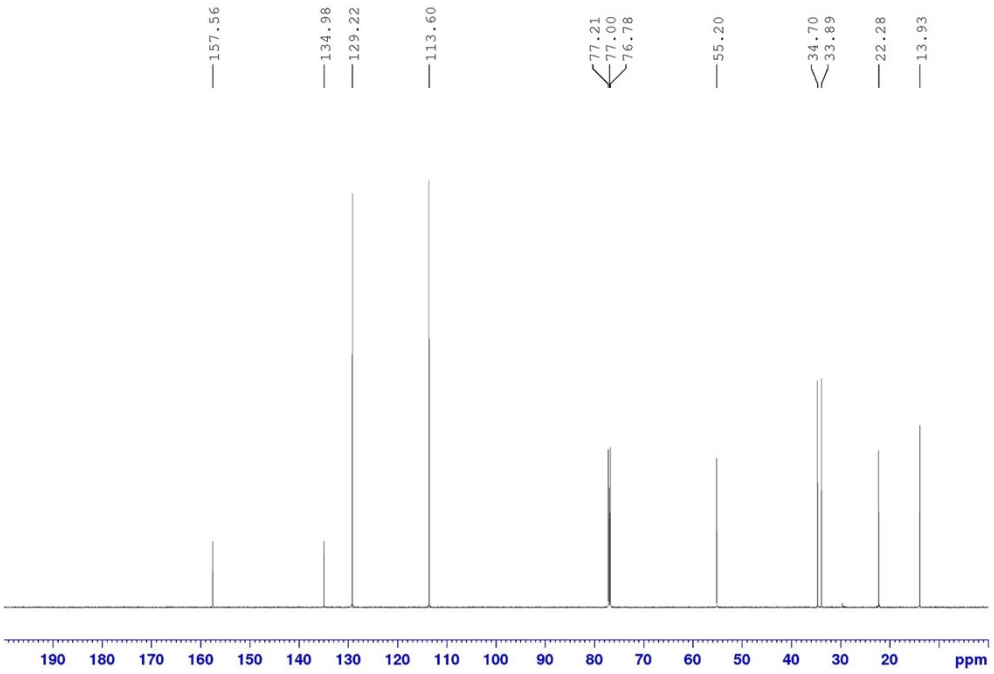
157.56
134.98
129.22
113.60
77.21
77.00
76.78
55.20
34.70
33.89
22.28
13.93
190 180 170 160 150 140 130 120 110 100 90 80 70 60 50 40 30 20 ppm

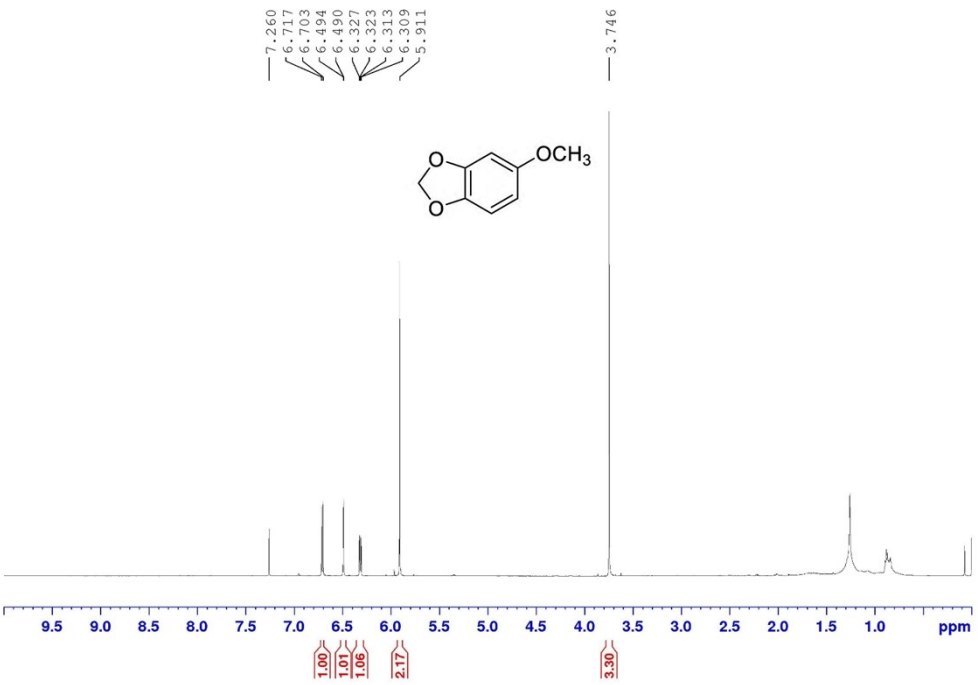
7.260
6.717
6.703
6.494
6.490
6.327
6.323
6.313
6.309
5.911
3.746
OCH3
O
O
9.5 9.0 8.5 8.0 7.5 7.0 6.5 6.0 5.5 5.0 4.5 4.0 3.5 3.0 2.5 2.0 1.5 1.0 ppm
1.00
1.01
1.06
2.17
3.30

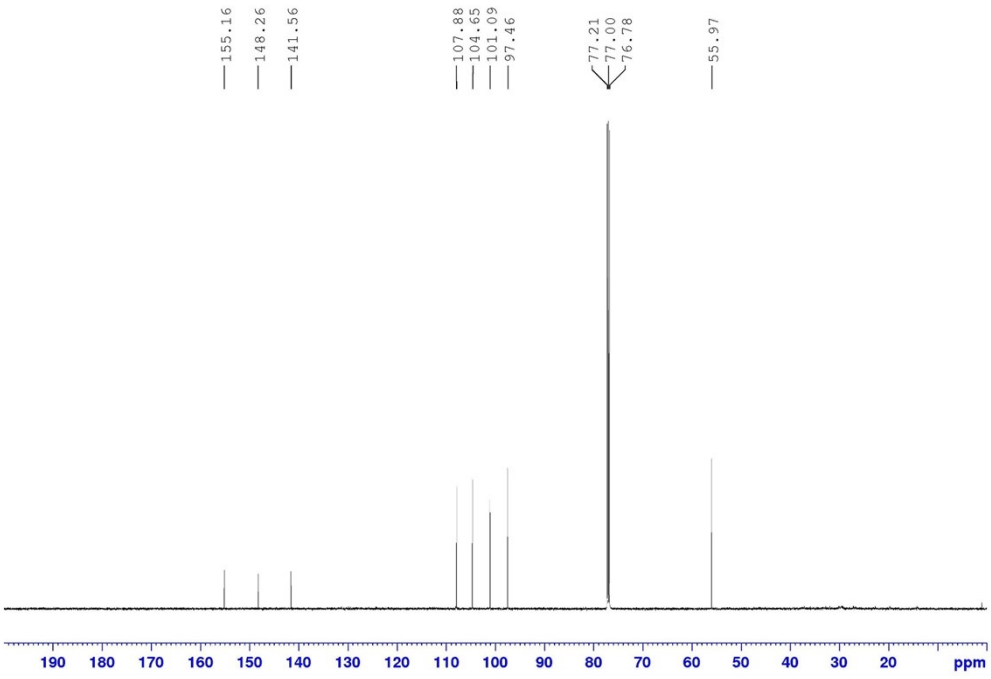
155.16
148.26
141.56
107.88
104.65
101.09
97.46
77.21
77.00
76.78
55.97
190 180 170 160 150 140 130 120 110 100 90 80 70 60 50 40 30 20 ppm

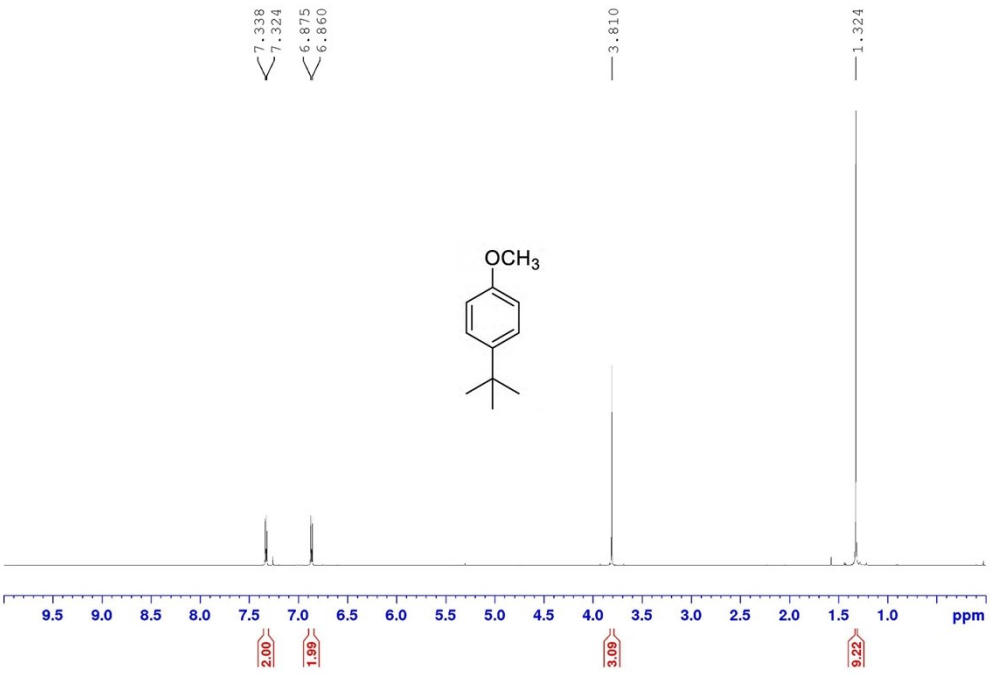
7.338
7.324
6.875
6.860
3.810
1.324
OCH3
9.5 9.0 8.5 8.0 7.5 7.0 6.5 6.0 5.5 5.0 4.5 4.0 3.5 3.0 2.5 2.0 1.5 1.0 ppm
2.00
1.99
3.09
9.22

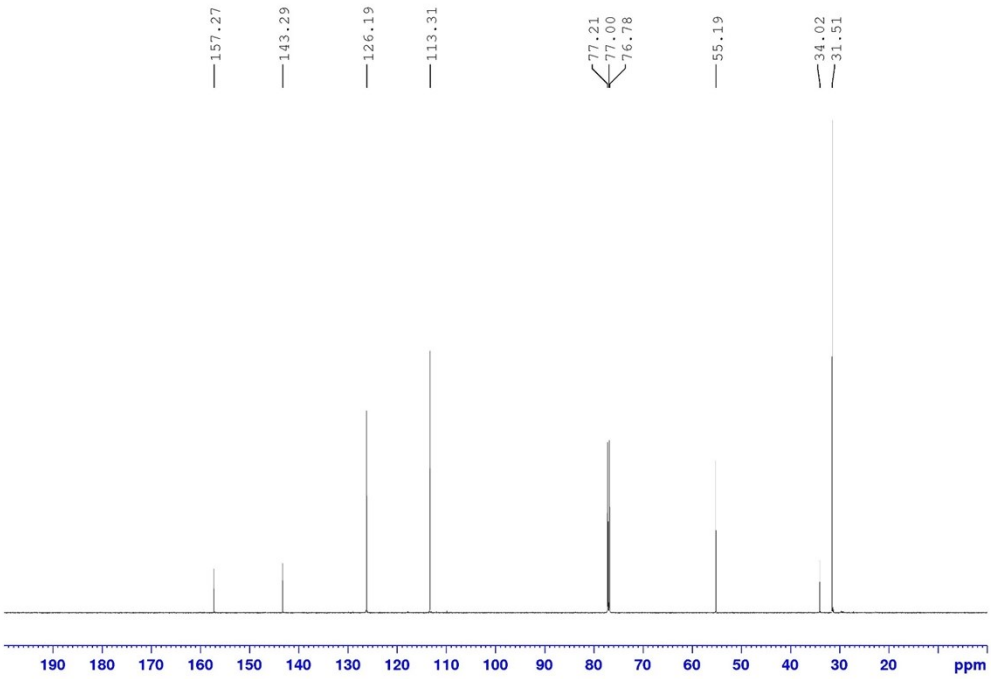
157.27
143.29
126.19
113.31
77.21
77.00
76.78
55.19
34.02
31.51
190 180 170 160 150 140 130 120 110 100 90 80 70 60 50 40 30 20 ppm

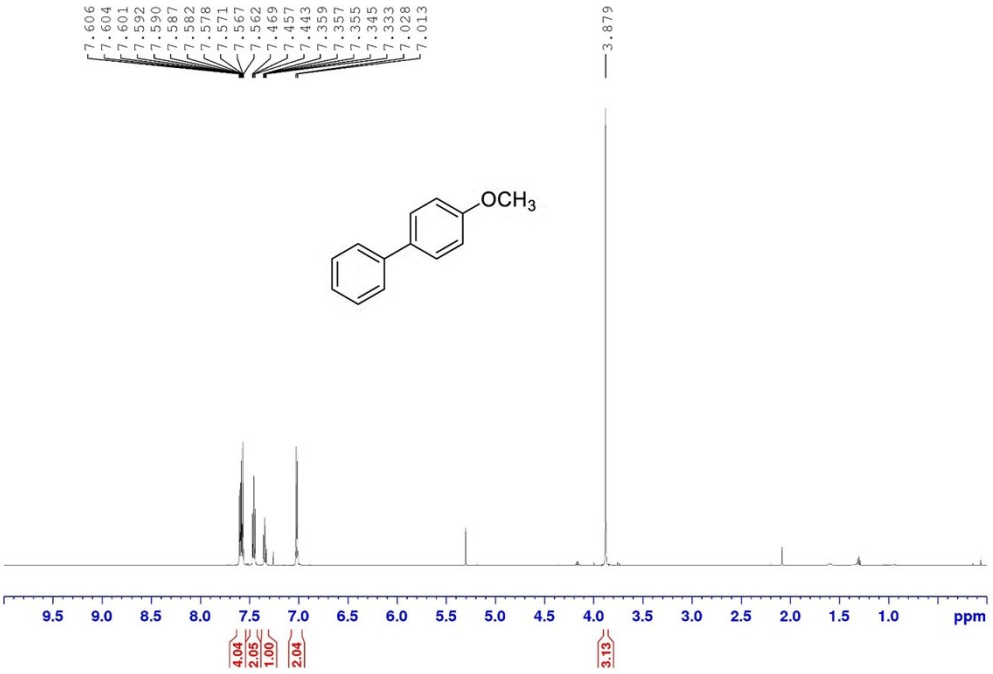
7.606
7.604
7.601
7.592
7.590
7.587
7.582
7.578
7.571
7.567
7.562
7.469
7.457
7.443
7.359
7.357
7.355
7.345
7.333
7.028
7.013
3.879
OCH3
9.5 9.0 8.5 8.0 7.5 7.0 6.5 6.0 5.5 5.0 4.5 4.0 3.5 3.0 2.5 2.0 1.5 1.0 ppm
4.04
2.05
1.00
2.04
3.13

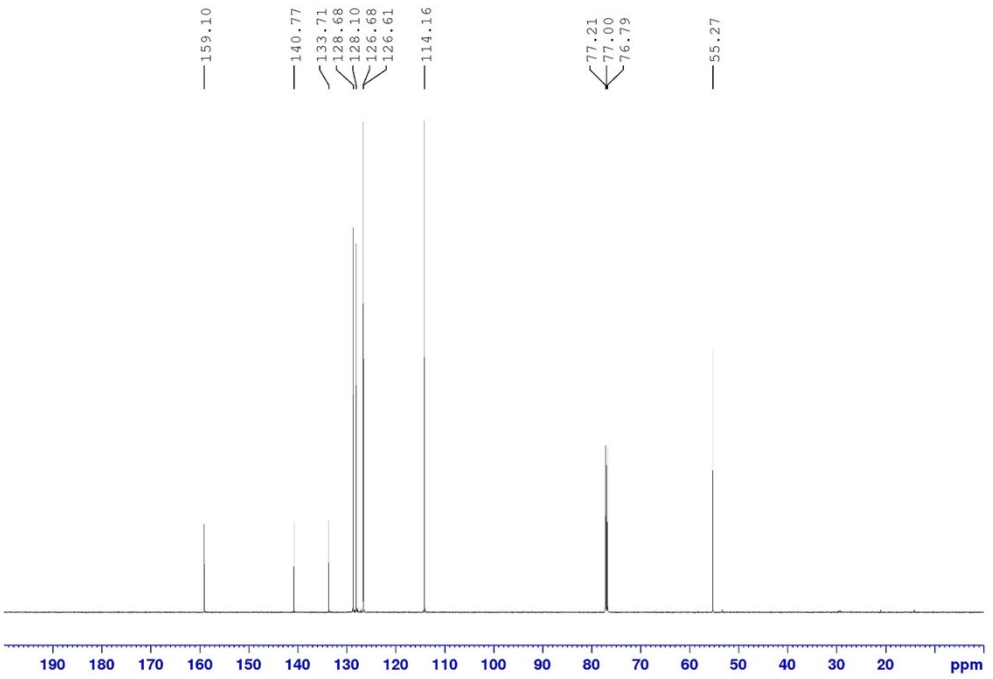
159.10
140.77
133.71
128.68
128.10
126.68
126.61
114.16
77.21
77.00
76.79
55.27
190 180 170 160 150 140 130 120 110 100 90 80 70 60 50 40 30 20 ppm

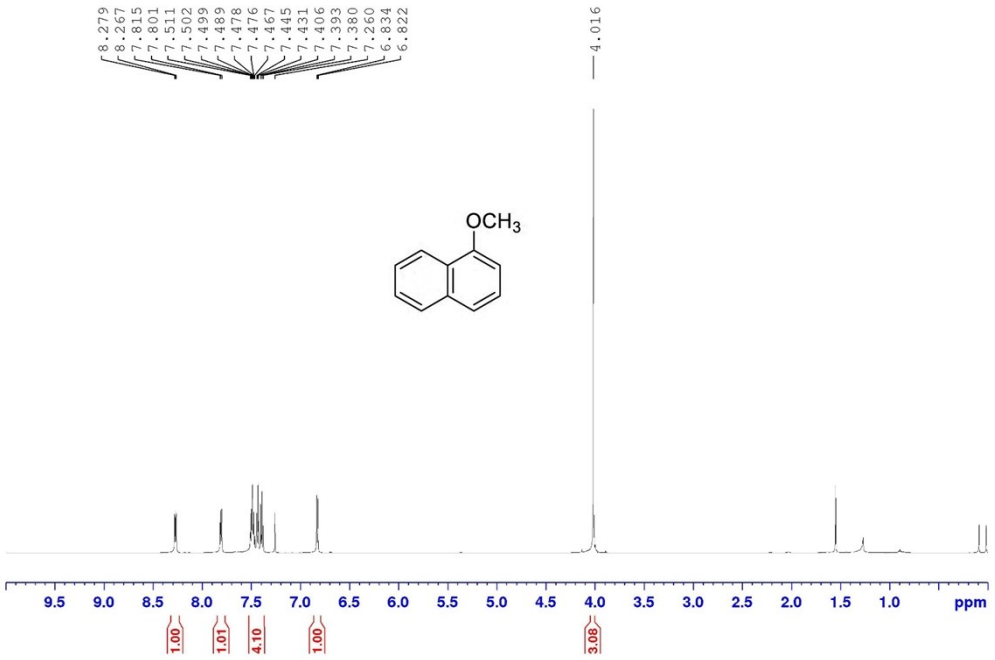
8.279
8.267
7.815
7.801
7.511
7.502
7.499
7.489
7.478
7.476
7.467
7.445
7.431
7.406
7.393
7.380
7.260
6.834
6.822
4.016
OCH3
9.5 9.0 8.5 8.0 7.5 7.0 6.5 6.0 5.5 5.0 4.5 4.0 3.5 3.0 2.5 2.0 1.5 1.0 ppm
1.00
1.01
4.10
1.00
3.08

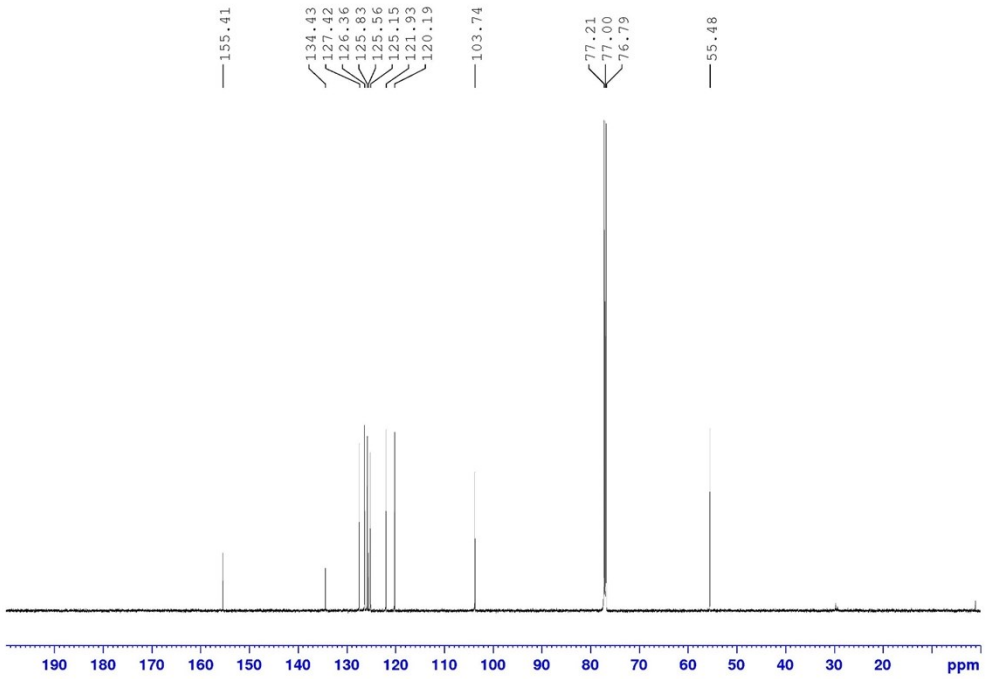
155.41
134.43
127.42
126.36
125.83
125.56
125.15
121.93
120.19
103.74
77.21
77.00
76.79
55.48
190 180 170 160 150 140 130 120 110 100 90 80 70 60 50 40 30 20 ppm

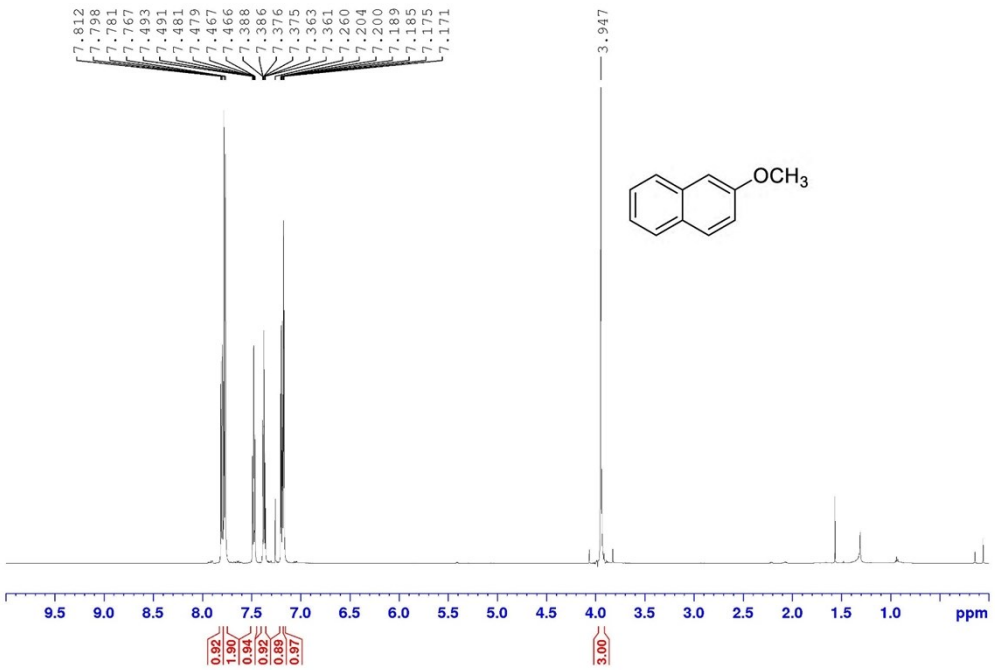
7.812
7.798
7.781
7.767
7.493
7.491
7.481
7.479
7.467
7.466
7.388
7.386
7.376
7.375
7.363
7.361
7.260
7.204
7.200
7.189
7.185
7.175
7.171
3.947
OCH3
9.5 9.0 8.5 8.0 7.5 7.0 6.5 6.0 5.5 5.0 4.5 4.0 3.5 3.0 2.5 2.0 1.5 1.0 ppm
0.92
1.90
0.94
0.92
0.89
0.97
3.00

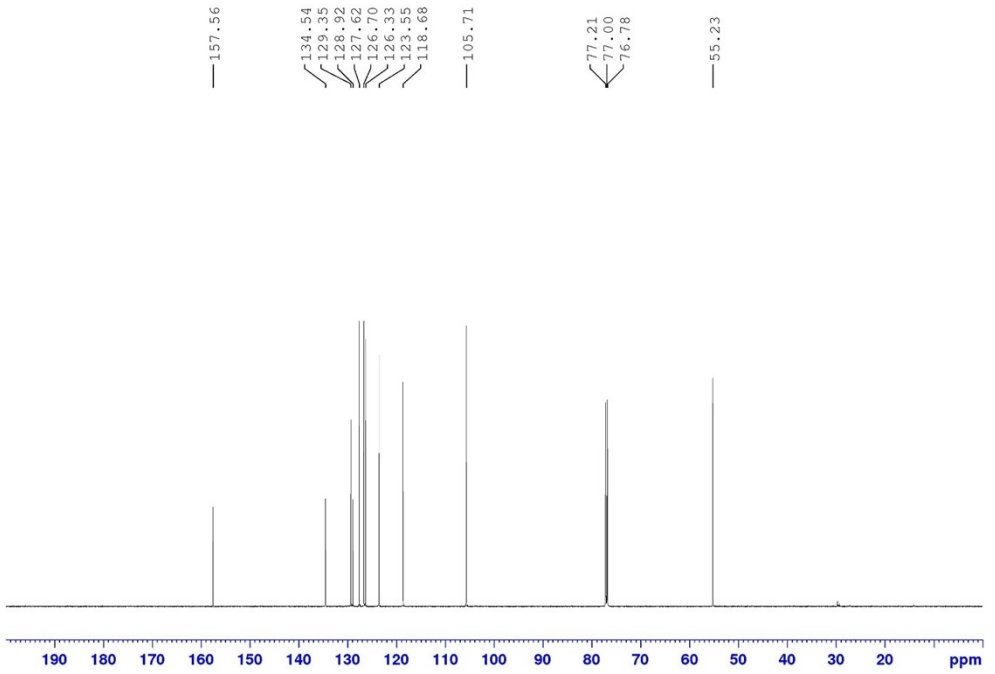
157.56
134.54
129.35
128.92
127.62
126.70
126.33
123.55
118.68
105.71
77.21
77.00
76.78
55.23
190 180 170 160 150 140 130 120 110 100 90 80 70 60 50 40 30 20 ppm

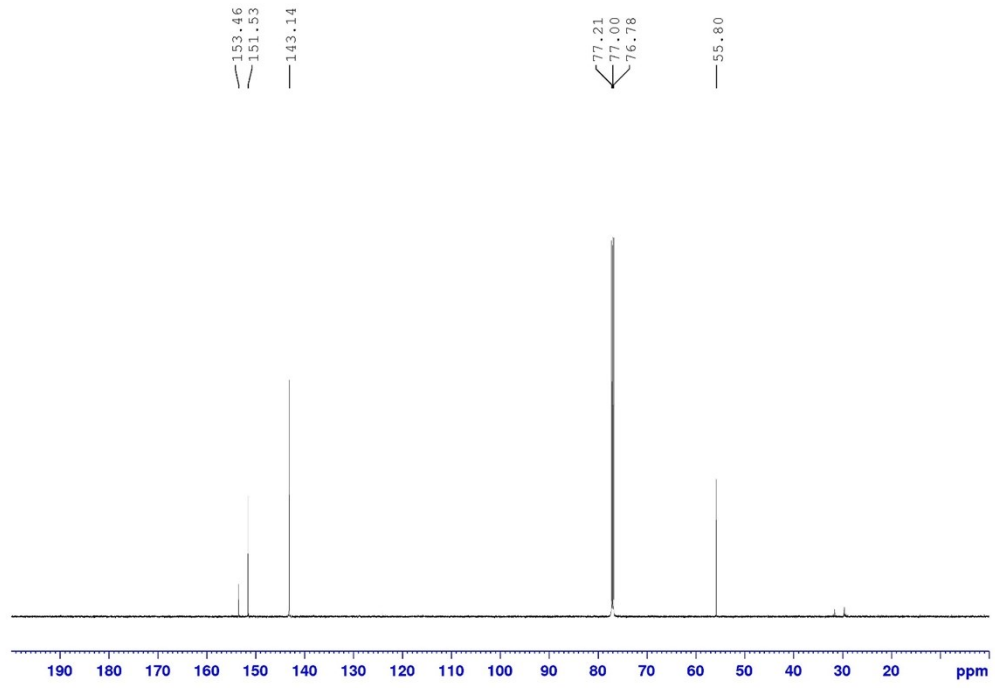
153.46
151.53
143.14
77.21
77.00
76.78
55.80
190 180 170 160 150 140 130 120 110 100 90 80 70 60 50 40 30 20 ppm

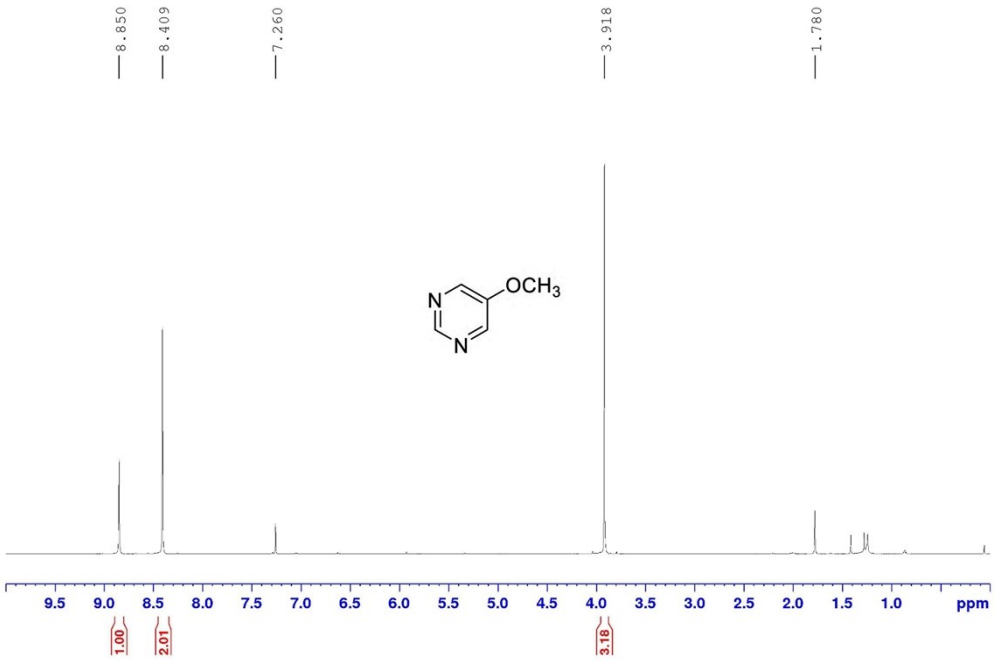
8.850
8.409
7.260
3.918
1.780
OCH3
N
N
9.5 9.0 8.5 8.0 7.5 7.0 6.5 6.0 5.5 5.0 4.5 4.0 3.5 3.0 2.5 2.0 1.5 1.0 ppm
1.00
2.01
3.18

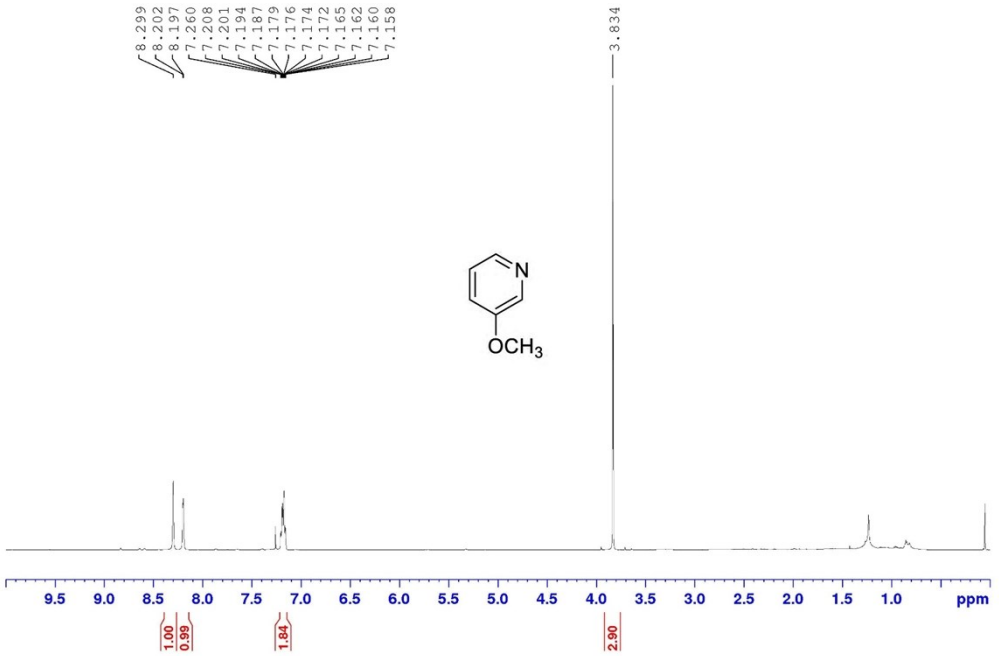
8.299
8.202
8.197
7.260
7.208
7.201
7.194
7.187
7.179
7.176
7.174
7.172
7.165
7.162
7.160
7.158
3.834
N
OCH3
9.5 9.0 8.5 8.0 7.5 7.0 6.5 6.0 5.5 5.0 4.5 4.0 3.5 3.0 2.5 2.0 1.5 1.0 ppm
1.00
0.99
1.84
2.90

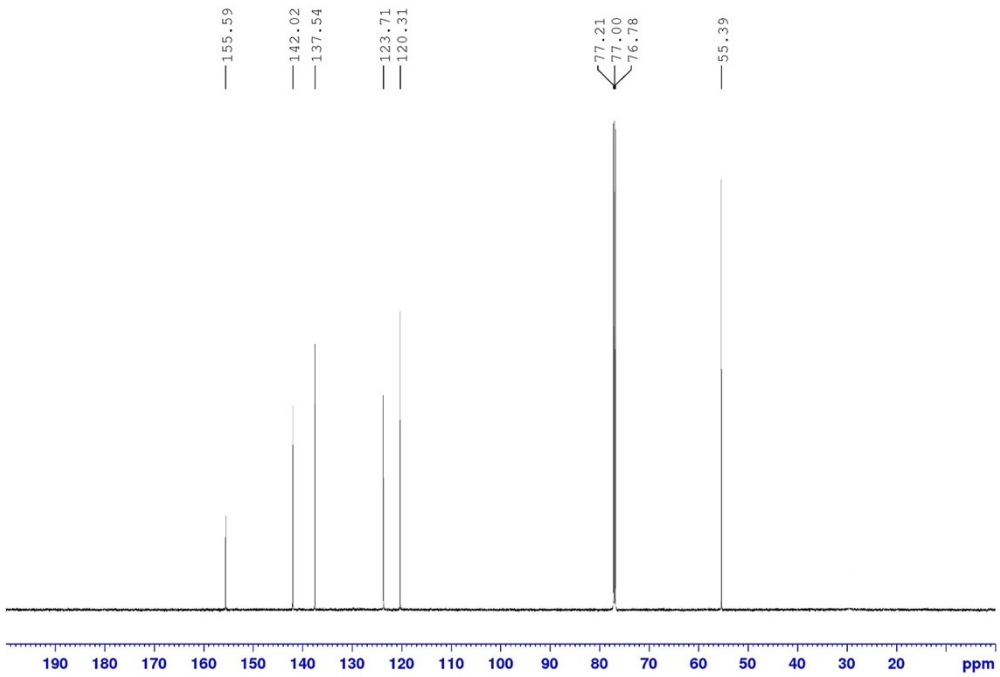
155.59
142.02
137.54
123.71
120.31
77.21
77.00
76.78
55.39
190 180 170 160 150 140 130 120 110 100 90 80 70 60 50 40 30 20 ppm